Research Article

Phylogenomics of Perityleae (Compositae) provides new insights into morphological and chromosomal evolution of the rock daisies

Isaac H. Lichter-Marck[1]* (iD), William A. Freyman[1], Carolina M. Siniscalchi[2] (iD), Jennifer R. Mandel[3] (iD), Arturo Castro-Castro[4], Gabriel Johnson[5], and Bruce G. Baldwin[1]

[1]Department of Integrative Biology and Jepson Herbarium, University of California, Berkeley, CA 94720, USA
[2]Department of Biological Sciences, Mississippi State University, Mississippi State, MS 39762, USA
[3]Department of Biological Sciences, Center for Biodiversity Research, University of Memphis, Memphis, TN 38152, USA
[4]Centro Interdisciplinario de Investigacion para el Desarrollo Integral Regional Unidad Durango, Durango, Durango, Mexico
[5]Department of Botany, MRC-166, National Museum of Natural History, Smithsonian Institution, PO Box 37012 Washington, DC 20013-7012, USA
*Author for correspondence. E-mail: ilichtermarck@berkeley.edu
Received 14 July 2020; Accepted 29 November 2020; Article first published online 04 December 2020

Abstract   Rock daisies (Perityleae; Compositae) are a diverse clade of seven genera and ca. 84 minimum-rank taxa that mostly occur as narrow endemics on sheer rock cliffs throughout the southwest United States and northern Mexico. Taxonomy of Perityleae has traditionally been based on morphology and cytogenetics. To test taxonomic hypotheses and utility of characters emphasized in past treatments, we present the first densely sampled molecular phylogenies of Perityleae and reconstruct trait and chromosome evolution. We inferred phylogenetic trees from whole chloroplast genomes, nuclear ribosomal cistrons, and hundreds of low-copy nuclear genes using genome skimming and target capture. Discordance between sources of molecular data suggests an underappreciated history of hybridization in Perityleae. Phylogenies support the monophyly of subtribe Peritylinae, a distinctive group possessing a four-lobed disc corolla; however, all of the phylogenetic trees generated in this study reject the monophyly of the most species-rich genus, *Perityle,* as well as its sections: *Perityle* sect. *Perityle, Perityle* sect. *Laphamia,* and *Perityle* sect. *Pappothrix.* Using reversible jump MCMC, our results suggest that morphological characters traditionally used to classify members of Perityleae have evolved multiple times within the group. A base chromosome number $x = 9$ gave rise to higher base numbers in subtribe Peritylinae ($x = 12, 13, 16, 17, 18,$ and 19) through polyploidization, followed by ascending or descending dysploidy. Most taxa constitute a monophyletic lineage with a base chromosome number of $x = 17$, with multiple neo-polyploidization events. These results demonstrate the advantages and obstacles of next-generation sequencing approaches in synantherology while laying the foundation for taxonomic revision and comparative study of the evolutionary ecology of Perityleae.

Key words: chromosome evolution, Compositae, genome skimming, Heliantheae, Hyb-Seq, molecular systematics, morphological evolution, Perityleae, phylogenomics.

1 Introduction

The sunflower and daisy family (Compositae) is one of the most diverse plant families on Earth and is distinguished by a unique assemblage of floral and fruit traits. These characteristics include flowers (florets) joined into a capitulum, secondary pollen presentation by an exserted style passing through a fused anther tube, or "synanther," ovaries with a single basal ovule, and fruits that possess a modified calyx (pappus) (Anderberg et al., 2007; Funk et al., 2009a; Mandel et al., 2019). For most of the history of synantherology (the study of Compositae), floral and fruit morphology has formed the basis for classification of broad taxonomic groups (Cassini, 1829; Robinson, 1981; Bonifacino et al.,

2009; Heywood, 2009). In the present age of molecular systematics, however, new data have radically changed our understanding of deeper relationships in the family and put morphological characters that were previously given primacy in classification schemes into a new perspective (Baldwin et al., 2002; Panero & Funk, 2002, 2008). Now, phylogenomic approaches efficiently generating whole-genome sequence data are poised to extend the molecular revolution to shallower taxonomic scales, where once limited sampling and poor resolution, as well as conflicts between different sources of molecular data, have long impeded the reconstruction of evolutionary relationships (Mandel et al., 2014; Huang et al., 2016; Mandel et al., 2017;

Vargas et al., 2017; Pouchon et al., 2018; Herrando-Moraira et al., 2019; Siniscalchi et al., 2019; Thapa et al., 2020). With the rate and scale of the current biodiversity crises intensifying, refining and applying this modern molecular toolkit to Compositae systematics before the occurrence of significant extinction events is a primary challenge of 21st century synantherology.

One group of Compositae that has yet to receive focused molecular systematic study is the rock daisy tribe (Perityleae B.G. Baldwin), a diverse group of seven genera and ca. 84 currently recognized minimum-rank taxa that mostly occur as narrow endemics on the faces of sheer rock cliffs in semi-arid to arid mountain ranges throughout the southwest U.S. and northern Mexico (Fig. 1, Powell, 1969, 1972a, 1972b, 1973a, 1973b, 1974; Baldwin et al., 2002; Panero, 2007). Morphological characteristics of Perityleae include principally epaleate heads, tetramerous disc corollas, one or two series of subequal phyllaries, glandular foliage, and two- or four-sided phytomelanic cypselae, with or without a crown of pappus squamellae and from 0 to 35 barbed pappus bristles (Baldwin et al., 2002; Panero, 2007). Limited sampling of Perityleae using ITS data (Baldwin et al., 2002) and cpDNA data (Panero, 2007) provide support for monophyly of the tribe. Perityleae is nested within the Heliantheae alliance (Heliantheae Cass. s.l.) in recent family-wide phylogenomic studies, where it is the sister lineage to Eupatorieae Cass. (Mandel et al., 2019), a diverse (~2200 spp.) and distinctive tribe based in the Neotropics (Robinson et al., 2007).

Tribe Perityleae largely consists of the subtribe Peritylinae Rydb. sensu Robinson 1981 (four genera, 72 spp.), a group long recognized on the basis of its four-lobed disc corolla, an otherwise relatively rare trait among Heliantheae s.l. Subtribe Peritylinae is entirely restricted to western North America,

except for disjunct populations in South America assigned previously to *Perityle emoryi* Torr. (Powell, 1974). Two other subtribes are included in Perityleae: Lycapsinae H. Rob. and Galeaninae Panero & B.G. Baldwin. Lycapsinae contains one species, *Lycapsus tenuifolius* Phil. (Robinson, 1981; Baldwin et al., 2002), with a four-lobed disc corolla that is restricted to the barren Desventuradas archipelago of northern Chile. Galeaninae contains 2 genera and 11 spp. in Mexico and Central and South America. This subtribe was placed by Panero (2007) in Perityleae based on cpDNA data, and it differs from other members of the tribe in having five-lobed disc corollas.

Genera and sections of Perityleae (Table 1) have traditionally been delimited by morphological characters of the flower and fruit (Gray, 1852; Rydberg, 1914; Everly, 1947; Shinners, 1959) as well as cytogenetics (e.g., chromosome number variation) (Powell, 1968b; Powell & Sikes, 1970; Powell et al., 1975; Robinson, 1981). Important morphological traits include variation in the expression of ray florets, color of ray and disc corollas, pappus scales and bristles, ciliate or callous fruit margins, and the number of sides on the fruit (Niles, 1970; Powell, 1973a). The mosaic-like pattern and overlapping variation among these traits have led to considerable flux in generic circumscription, with successive taxonomists weighing differently the significance of particular fruit and flower traits (Powell, 1968a). In a series of papers, Turner and Powell treated Peritylinae, recognizing five genera: *Amauria* Benth., *Correllia* A.M. Powell, *Eutetras* A. Gray, *Pericome* A. Gray, and *Perityle* Benth (Turner, 1966; Powell, 1969, 1972a, 1973a, 1973b, 1974; Powell & Turner, 1974). One to three species constituted each of the first 4 genera and 65 spp. were included in the diverse genus *Perityle*, split among three infrageneric sections: *Perityle* sect. *Perityle*,
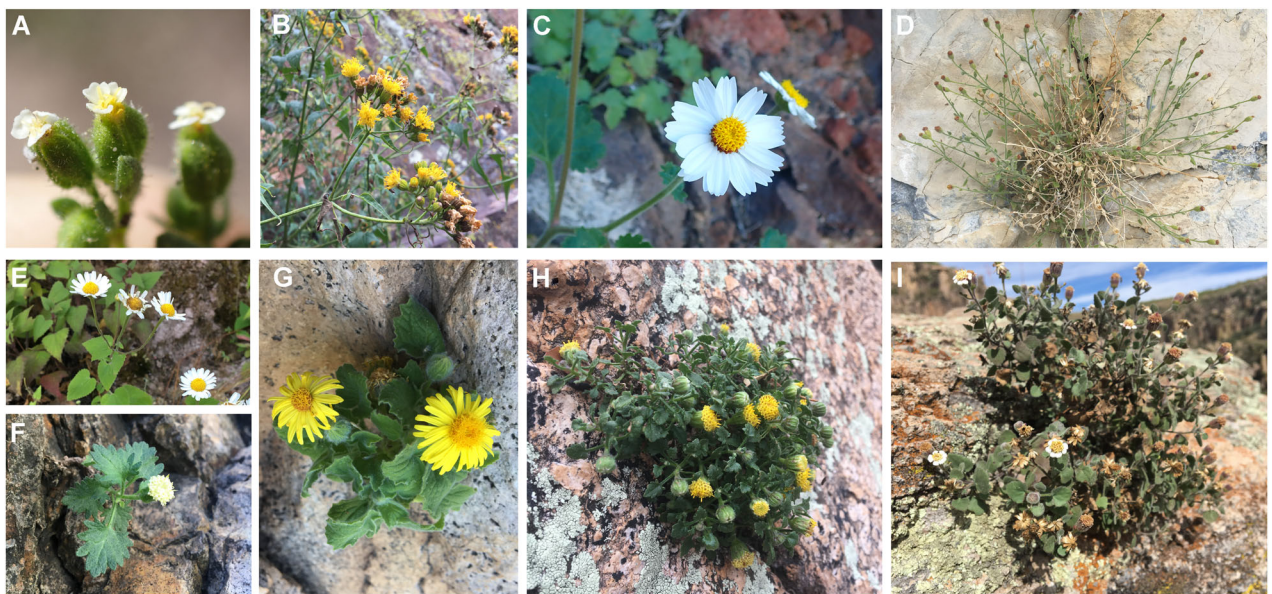

Fig. 1. Diversity in Perityleae, including representatives of prominent genera and sections sensu Yarborough & Powell (2006), Panero (2007), and Turner (2013). **A**, *Galeana pratensis* (Galeaninae). **B**, *Pericome caudata* (Peritylinae). **C**, *Amauria rotundifolia* (Peritylinae). **D**, *Perityle villosa* (*Perityle* sect. *Laphamia*). **E**, *Perityle turneri* (*Perityle* sect. *Perityle*). **F**, *Perityle rupestris* var. *albiflora* (*Perityle* sect. *Pappothrix*). **G**, *Perityle cordifolia* (*Perityle* sect. *Perityle*). **H**, *Perityle cochisensis* (*Perityle* sect. *Laphamia*). **I,** *Eutetras palmeri* (Peritylinae). Photos by ILM.

Table 1 Generic and infrageneric sections of the rock daisy tribe (Perityleae) after the most recent treatment by Powell (1968a, 1969, 1973a, 1974) including geographic distributions, chromosome numbers, morphological characters of the capitula, and life history and ecology

Taxa	Distribution	Chromosome number	Capitular characteristics	Life history and ecology
Perityle sect. *Pappothrix* (A. Gray) A.M. Powell	Northern Chihuahuan desert (southwest Texas & New Mexico).	$x = 17$ ($n = 17, 34, 68$)	Discoid or radiate with yellow ray corollas. Disc corollas yellow or white, 4-lobed. Fruit margins smooth. Pappus of 8–35 bristles, without scales.	Subshrubs with a woody caudex rooted in crevices of igneous and limestone rocks at mid to high altitude in arid mountain ranges.
Perityle sect. *Laphamia* (A. Gray) A.M. Powell	Southwest United States and Sonora, MX. Found in Sonoran, Great Basin, and Chihuahuan deserts.	$x = 17$ ($n = 17, 34, 51$)	Discoid or radiate with yellow ray corollas. Disc corollas yellow or white, 4-lobed. Cypselae 2-sided. Pappus of (0)1–4 bristles and a reduced crown of scales.	Subshrubs with a woody caudex rooted in crevices of igneous and limestone rocks in canyons and arid mountain ranges.
Perityle sect. *Perityle*	Southwest United States and northern Mexico, including Baja California. Also present in northern Chile. Prominent in the Sierra Madre Occidental of northwestern Mexico.	$x = 11, 12, 13, 16, 17, 19$	Radiate or discoid with yellow or white ray corollas. Disc corollas yellow, 4-lobed. Cypselae 2-sided. Fruit margins callous or ciliate. Pappus of (0) 1–2, bristles, and a corona of scales.	Annuals, perennials, or subshrubs in rocky crevices or soil. Low elevation deserts or arid to semi-arid sites in mid to high elevation desert mountain ranges.
Pericome A.Gray	Montane southwestern United States and northwestern Mexico.	$x = 18$	Discoid with yellow, 4-lobed corollas. Cypselae 2-sided. Fruit margins ciliate. Pappus of scales and (0)1–4 bristles.	Shrubs of arid rocky sites in mid to high elevation montane habitats.
Amauria Benth.	States of Baja California and Baja California Sur, MX and offshore islands.	$x = 18$	Radiate with white ray corollas and yellow, 4-lobed disc corollas. Cypselae 4-sided. Epappose.	Annuals or subshrubs in rocky crevices or soil in low desert.
Eutetras A. Gray	Bajillo region of central Mexico in the states of Jalisco, Aguascalientes, San Luis Potosi, and Queretaro.	$x = 18$	Radiate with white ray corollas. Disc corollas white or yellow, 4-lobed. Cypselae 4-sided. Pappus of four bristles and broad scales.	Perennial subshrubs in rock crevices in mid-elevation Chihuahuan desert.
Lycapsus Phil.	Desventuradas islands, Chile	Chromosome number unknown	Radiate with white ray corollas and yellow, 4-lobed disc corollas. Paleae present.	Perennial subshrub on rocky slopes.
Galeana La Llave	Mexico and Central America	$x = 9$	Radiate with white ray corollas and yellow, 5-lobed disc corollas. Disc cypselae 4-sided, ray cypselae 2-sided with broadly callous margins. Epappose.	Annuals in soil in semi-arid margins of desert and tropical dry forest.

Table 1 Continued

Taxa	Distribution	Chromosome number	Capitular characteristics	Life history and ecology
Villanova Lag.	Mexico and South America	$x = 10, 20$	Radiate with white ray corollas and yellow, 5-lobed disc corollas, ray cypselae 3-sided, disc cypselae 3–4-sided. Epappose.	Annual or short-lived perennial herbs in soil in tropical forest understory.

Perityle sect. *Laphamia* (A. Gray) A.M. Powell, and *Perityle* sect. *Pappothrix* (A. Gray) A.M. Powell.

Since this most recent set of generic revisions (Powell, 1969, 1972a, 1973a, 1973b, 1974), botanical exploration has led to the discovery and description of many new, narrowly endemic taxa of Perityleae from remote areas throughout the southwest United States and northern Mexico (Powell, 1976, 1983; Todsen, 1974, 1983; Welsh & Neese, 1983; Turner, 1989; Spellenberg & Powell, 1990; Carrillo-Reyes, 2008), but, as of yet, no focused molecular phylogenetic studies have been carried out on the tribe. Limited sampling using nuclear ribosomal internal transcribed spacer (ITS) data by Baldwin et al. (2002) as part of a larger study of helenioid Heliantheae provided tentative support for Powell's proposed inter-generic relationships, with a more inclusive concept of *Perityle* to encompass the monotypic genus *Correllia*. The low internal branch support found by Baldwin et al. (2002), however, highlights the key problem of lack of phylogenetic resolution in this tribe based on few loci.

Genome skimming (Straub et al., 2012; Dodsworth, 2015) is a next-generation sequencing approach in which whole-genome DNA is fragmented and sequenced at shallow depths to assemble high-copy gene regions. Targeted regions include the bi-parentally inherited whole nuclear ribosomal cistron, including the internal, external, and non-transcribed spacers, and the non-recombinant, uniparentally inherited chloroplast genome. Both nuclear ribosomal DNA (nrDNA) and chloroplast DNA (cpDNA) have been important in the reconstruction of the evolutionary history of Compositae at various scales of taxonomic organization (e.g., Baldwin et al., 1991; Susanna et al., 1995; Baldwin et al., 2002; Panero & Funk, 2008; Panero et al., 2014), but they often pose challenges to systematists when conflicts arise between trees generated from different sources of data (Baldwin, 1997; Vargas et al., 2017; Pouchon et al., 2018). Cytonuclear incongruence is common in Compositae and can be caused by error in phylogenetic inference, ongoing gene flow among lineages, hybridization, and incomplete lineage sorting (ILS) (Rieseberg & Soltis, 1991; Maddison, 1997; Huelsenbeck et al., 2000; Vargas et al., 2017).

Target capture is a next-generation sequencing approach yielding sequences of pre-selected gene regions that is often used to target low-copy nuclear loci from across the genome for phylogenetics (Smith et al., 2014; Weitemier et al., 2014). Here, RNA-based probes are specifically designed to hybridize with and capture putatively orthologous gene regions. The Compositae conserved ortholog set (COS) for phylogenetic study of Compositae pioneered by Mandel et al. (2014, 2015, 2017) has been used to elucidate family-wide relationships (Mandel et al., 2019; Watson et al., 2020), within tribes (Herrando-Moraira et al., 2019; Siniscalchi et al., 2019), and, increasingly, within genera (Thapa et al., 2020; Acker-field et al., pers. comm.). Given the family's history of large-scale gene duplications and polyploidy (Barker et al., 2016; Huang et al., 2016), intensive quality control and filtering of data are necessary, including strict filtering of gene sequences suspected of being paralogs (Jones et al., 2019; Siniscalchi et al., 2019). Refining this target-capture approach for Compositae to produce highly supported phylogenies with minimal data discarded during quality control has been an ongoing challenge.

Phylogenetic relationships within Perityleae hold important implications not only for taxonomy, but also for evaluating the evolutionary dynamics of floral and fruit traits in the group and elsewhere. Characters such as corolla color and type, patterns of seed-coat thickening, receptacular bract (or chaff) occurrence, types of pappus elements, pollen ornamentation, and the structure of anthers and style branches have often been emphasized in Compositae systematics. At the same time, the evolutionary lability of floral and fruit traits in composites is perceived to have been an important factor in the widespread ecological success of the family (Stuessy & Garver, 1994; Funk et al., 2009b; Panero & Crozier, 2016; Mandel et al., 2019). Pappus elements are particularly multi-functional, aiding in dispersal, as well as protecting against herbivores and desiccation (Robinson, 1981; Mandel et al., 2019), with rapid loss or reduction of the pappus commonly associated with isolation on islands or island-like habitats. Loss of dispersal ability on islands is well documented in Compositae and is thought to occur due to strong selection against dispersal away from a suitable habitat (Carlquist, 1974; Cody & Overton, 1996; Jeffrey, 2007). As most Perityleae are restricted to island-like rock habitats, they provide a biogeographically important system for reconstructing the evolution of taxonomically important fruit and flower traits to understand if they have been conserved or labile over time.

Whole-genome duplications and chromosome number evolution have recently been implicated as important correlates of rapid diversification events in Compositae (Barker et al., 2016; Huang et al., 2016; Panero & Crozier, 2016). Similar to many other higher taxa of the Heliantheae alliance, Perityleae shows an extreme diversity of chromosome numbers, ranging from 9 to 68 pairs

J. Syst. Evol. 58(6): 853–880, 2020

www.jse.ac.cn

(Robinson et al., 1981). Powell (1968b, 1970) completed hundreds of chromosome counts as part of his monographic research on Perityleae, but the abundance of data amassed by him has yet to be explicitly reconstructed on a phylogeny. Powell predicted a base chromosome number of $x = 18$ for subtribe Peritylinae and hypothesized that dysploid decreases and whole-genome duplications were the main processes leading to contemporary chromosome number variation. Recent advances in model-based methods make it possible to quantitatively test Powell's longstanding cytogenetic hypotheses about Perityleae (Mayrose et al., 2010; Glick & Mayrose, 2014; Freyman & Höhna, 2018).

Aiming to clarify relationships among members of Perityleae and to gain a new perspective on the evolution of morphological and cytogenetic characters previously utilized in taxonomic work, we present the first densely sampled phylogenies of Perityleae from whole ribosomal and chloroplast DNA, as well as hundreds of low-copy nuclear loci. In doing so, we investigate the effectiveness of genome skimming and target-capture approaches and examine relative congruence between trees inferred from different linkage groups in the genome. To understand evolutionary changes in floral and fruit morphology and chromosome numbers, we reconstruct ancestral states of these traits. The extreme ecological specialization for life on sheer rock cliffs exhibited by many taxa in Perityleae makes this an excellent group for studying evolutionary diversification in an arid environment. Thus, this study provides the foundation for finer scale investigations to follow into this fascinating tribe of composites.

2 Material and Methods

2.1 Sampling
We sampled leaf tissue for DNA extraction from individuals of all recognized minimum-rank taxa in subtribe Peritylinae (Panero, 2007), except for *Pericome macrocephala* B.L. Rob., *Perityle aurea* Rose, *Perityle grandiflora* Brandegee, *Perityle lloydii* B.L. Rob. & Fernald, *Perityle pennelli* B.L. Turner, *Perityle scopulorum* (M.E. Jones) A.M. Powell & B.L. Turner, and *Perityle warnocki* A.M. Powell (material unattainable). For subtribe Lycapsinae (Panero, 2007), attempts to obtain a suitable leaf tissue for DNA analysis of *Lycapsus tenuifolius* from the Desventuradas Islands are still ongoing. Two representative samples from each genus in subtribe Galeaninae (Panero, 2007) were included for DNA extraction, *Galeana pratensis* (Kunth) Rydb. and *Villanova achilleoides* (Less.) Less.; however, only *G. pratensis* yielded an extract of sufficiently high quality to be included in our analyses. Five taxa of tribe Eupatorieae were included as the outgroup [*Chromolaena corymbosa* (Aubl.) R.M. King & H. Rob., *Conoclinium coelestinum* (L.) DC., *Eutrochium fistulosum* (Barratt) E.E. Lamont, *Pleurocoronis pleuriseta* (A. Gray) R.M. King & H. Rob., and *Stevia* sp.] as well as *Helianthus annuus* L. of tribe Heliantheae s.s. For accession numbers and corresponding herbaria for specimens used in this study, see Appendix I.

The leaf tissue was sampled from field collections and herbarium specimens at ARIZ, CAS, LL/TEX, NY, SD, SRSC, UC/JEPS, UCR, & US. When possible, we sampled from type

specimens or from vouchers annotated by A. Michael Powell; however, all specimens were carefully examined to ensure that identifications corresponded with current taxonomy (e.g., Yarborough & Powell, 2006; Turner, 2013). Due to the remote nature and inaccessibility of Perityleae habitats, many taxa are known from few or only a single collection(s). Much effort in this study has, therefore, been dedicated to document new populations of poorly known taxa and sampling from field-collected, silica-dried samples following best practices (Funk et al., 2018).

2.2 DNA extraction, library preparation, and sequencing
We extracted DNA from ground leaf fragments using the DNeasy Plant Mini Kit (Qiagen, Valencia, CA, USA) or a modified version of Doyle and Doyle's (1987) CTAB protocol (adding Proteinase K to the initial lysis buffer, adding a chloroform: isoamyl alcohol extraction step, and extending the precipitation step to 1–12 h). If needed, samples were further purified using Qiagen filter columns to remove coprecipitated polysaccharides. Molecular work was performed in the Baldwin lab in the Department of Integrative Biology, the Molecular Phylogenetics Laboratory of the University and Jepson Herbaria, the Evolutionary Genetics Laboratory in the Museum of Vertebrate Zoology at UC Berkeley, and the Laboratory of Analytical Biology at the Smithsonian Institution's National Museum of Natural History in Washington, DC.

DNA extracts were diluted and fragmented using a QSonica at 25% amplitude, 10-10 pulse for 7 min, shearing DNA to 400–500 bp, excepting herbarium samples showing prior fragmentation from age, for which we skipped this step. For DNA sequencing on Illumina platforms, 250–500 ng of DNA, as quantified using a Qubit dsDNA BR (broad range) Assay Kit (Thermo Fisher Scientific, Waltham, MA, USA), was prepared using the NEBnext Ultra II DNA Library Prep Kit for Illumina (New England Biolabs, Ipswich, MA, USA) according to the manufacturer's instructions, except for extending the final PCR reaction to 16 cycles. Samples were dual indexed using iTru adapters (Glenn et al., 2019).

To capture low-copy gene regions previously shown to be useful for phylogenetics in the Compositae (Mandel et al., 2014), we enriched a subset of libraries derived from field-collected material for target capture using the myBaits COS Compositae-1061 1kv1 bait set (Arbor Biosciences, Ann Arbor, MI, USA) developed by Mandel et al. (2014, 2015, 2017). Samples were enriched for 42 h at 62°C, followed by amplification for 10–16 cycles or until concentrations of enriched DNAs were detectable on an agarose gel. We spiked our final DNA pools with 20% unenriched library for genome skimming of nrDNA and cpDNA (Straub et al., 2012; Smith et al., 2014). Multiplexed samples were submitted for paired-end sequencing on two lanes of an Illumina HiSeq 4000 system (Illumina inc., San Diego, CA, USA). More details on the targets and methods used can be found in Mandel et al. (2014, 2015, 2017).

2.3 Sequence assembly and mapping
Illumina adapter sequences were removed, and the raw sequence reads were quality filtered using Trimmomatic v0.36 (Bolger et al., 2014). Reads were trimmed when the average Phred quality score in a 10-bp sliding window was

less than 20. Reads that were less than 40 bp or that did not survive the filtering process in both forward and reverse directions were excluded.

To assemble sequence fragments on whole plastomes (cpDNA) and nuclear ribosomal cistrons (nrDNA), we used the Burroughs–Wheeler Aligner (BWA; Li & Durbin, 2010) with the *Helianthus annuus* whole chloroplast genome sequence (GenBank accession number KM360047) as a scaffold. Nuclear ribosomal DNA was assembled along a hybrid reference sequence composed of an 18S through 26S DNA sequence from *Perityle emoryi* (GenBank accession number AF374868.1) flanked by external transcribed spacer (ETS) and the non-transcribed spacer (NTS) from the *Helianthus annuus* whole ribosomal cistron sequence (GenBank accession number KF767534.1).

Additionally, we used SPAdes (Bankevich et al., 2012) for de novo assembly of sequence reads into contigs with k-mer lengths of 21, 33, 55, 77, 99, and 127. Resultant contigs were matched back to target sequences for low-copy nuclear loci using the PHYLUCE pipeline (Faircloth, 2016), which generated individual matrices for each of the original targeted regions. To balance possible sources of noise from missing data with statistical support, we used the "phyluce_align_get_only_taxa_with_min_loci" function to generate two subsets of alignments in which at least 50% and 75% of taxa were represented. Data matrices were aligned using MAFFT (Katoh et al., 2009) and aberrant sequences and patchy regions were removed using trimAl using the default settings (Capella-Gutiérrez et al., 2009).

2.4 Phylogenetic methods

Phylogenetic analyses were performed separately for data matrices containing aligned whole chloroplast genomes, nuclear ribosomal cistrons, and a concatenated matrix composed of 212 low-copy nuclear loci. Phylogenetic trees based on maximum likelihood were inferred using RAxML (Stamatakis, 2014) on XSEDE through the CIPRES Science Gateway portal (Miller et al., 2010) using the GTRCAT model of molecular substitution and 1000 rapid bootstrap replicates. Phylogenetic trees were also inferred using Bayesian approaches in RevBayes (Höhna et al., 2016). A constant rate birth–death process was used as a tree prior and molecular substitution was modeled with a GTR + gamma + I model with four discrete rate categories. An approximation of the posterior distribution of trees was obtained during 30 000 generations of a Markov Chain Monte Carlo (MCMC) method. The MCMC was inspected for stationarity and sufficient effective sample sizes in the software program Tracer (Rambaut et al., 2018). Additionally, to account for potential gene tree discordance due to ILS, we used the software program ASTRAL-III (Zhang et al., 2018) to infer a species tree. For this analysis, we inferred individual gene trees for 212 low-copy nuclear loci using RAxML with 100 bootstrap replicates under a GTRCAT model of molecular substitution. Nodes with a bootstrap value lower than 0.2 were collapsed.

To investigate congruence among phylogenies based on separate sources of data, we inferred trees for a subset of taxa found in all three data sets and then compared discordance visually. Quantitative measurements of congruence between species trees were obtained using the function treedist in the R package phangorn (Schliep, 2011),

which measures Robinson–Foulds, branch score, path, and quadratic path distances between trees. After inspecting trees based on different sources of molecular data for congruence, we carried out a combined phylogenetic analysis of nuclear ribosomal cistrons and low-copy nuclear loci. The combined analysis was carried out using Bayesian inference in RevBayes (Höhna et al., 2016), as described above. To account for variation in the molecular substitution process in different sources of data, we partitioned our analysis by gene locus and independently inferred process parameters for each partition.

2.5 Ancestral state reconstructions

Variation in morphological traits of flowers and fruits among study taxa was compiled from taxonomic treatments (Turner, 1966; Powell, 1969, 1972a, 1973a, 1973b, 1974, 1976; Powell & Turner, 1974) and species descriptions (Powell, 1983; Todsen, 1974, 1983; Welsh & Neese, 1983; Turner, 1989; Spellenberg & Powell, 1990; Carrillo-Reyes, 2008), supplemented with direct observations of herbarium samples. Morphological characters of the florets considered in this analysis included the presence or absence of ray florets, ray corolla color (yellow or white), and disc corolla color (yellow or white). Fruit characters included the presence or absence of pappus scales, callous or ciliate fruit margins, number of pappus bristles, and number of fruit sides. Given potential ambiguity in the interpretation of morphological traits, especially with respect to pappus elements, we adopted the explicit definitions emphasized in Powell's (1969, 1972a, 1973a, 1973b, 1974) taxonomic treatments. Pappus scales referred specifically to a crown of broad to laciniate, erect pappus squamellae; callous margins referred to thick, raised, rough, or corky-papery edges on the cypselae margins; ciliate margins referred to long glandular or eglandular pilose indument, but not mere pubescence, along the cypselae margins; the number of fruit sides was determined by knowing whether the cypselae are two- or four-angled in cross-section; and the pappus bristle number referred to the approximate abundance of erect pappus bristles. To account for variability in pappus bristle count among individuals and among florets within an individual, we adopted the three categories used by Powell (1969, 1972a, 1973a, 1973b, 1974) to describe pappus bristle abundance in Perityleae: absence of bristles, presence of 1–4 erect bristles (most taxa), and the relatively rare condition of possessing a dense agglomeration of 10–35 bristles. For all morphological characters, when polymorphism was observed within taxa, we explicitly coded this into our morphological data by assigning multiple character states to a given taxon.

We estimated transition rates among character states and reconstructed ancestral traits using Bayesian model testing with reversible jump MCMC (Huelsenbeck et al., 2004) and stochastic character mapping (Huelsenbeck et al., 2003). Our analyses were implemented in RevBayes (Höhna et al., 2016) using the phylogenetic analysis of the combined nuclear ribosomal cistron and low-copy nuclear loci. To account for phylogenetic uncertainty, we based our analyses on the posterior distribution of 604 maximally supported phylogenetic trees generated by MCMC during Bayesian phylogenetic inference, and to account for incongruence between sources of molecular data, we replicated the analyses on a

posterior distribution of trees from our Bayesian phylogenetic analysis of the chloroplast genome. Outgroup taxa were pruned from each tree topology after rooting and dating of trees with the root() and chronos() function in the R package Phytools (Revell, 2012). A relaxed molecular clock with an uninformative root age prior of 1 was used to date the posterior distribution of trees.

We used reversible jump MCMC to estimate model-averaged transition rates between morphological character states while sampling from all plausible models of morphological evolution. The models of morphological change included all combinations of irreversible models, where one or more transition rates were fixed to zero, and a model of reversible change where transitions were independent and non-zero. Each of these models was assigned an equal prior probability and root state frequencies were estimated using a uniform Dirichlet prior. After performing a prior sensitivity analysis, we chose to draw non-zero transition rates from an exponential distribution with a mean of one expected character transition over the tree. Transition rate parameters were estimated and ancestral characters were mapped during 12 000 generations of reversible jump MCMC with a burnin of 1200 generations, after which the results were inspected for stationarity and an effective sample size greater than 500 in the software program Tracer (Rambaut et al., 2018). Model-averaged transition rate parameters and maximum a posteriori ancestral states were compiled from the posterior sample of stochastic character maps and illustrated on the MAP tree using the R package RevGadgets (https://github.com/revbayes/RevGadgets). We performed model fit comparisons independently for each transition rate by calculating Bayes factors as the ratio of the posterior odds of zero transition rates over non-zero parameter estimates. We interpreted a Bayes factor of less than 0.1 as strong support for irreversibility and greater than 0.9 as strong statistical support for reversible evolution.

Chromosome counts for Perityleae from microsporocytes or root apical meristems were compiled from the primary literature and the Chromosome Counts Database (Rice et al., 2015). Rates of dysploid chromosome gains and losses, as well as whole-genome duplications and demi-polyploidiziations, were inferred in the maximum likelihood-based software program ChromEvol (Glick & Mayrose, 2014). To account for incongruence between different sources of molecular data, the analysis was replicated for the tree based on a combined matrix of nrDNA and low-copy nuclear loci and for the tree based on the chloroplast genome. The Akaike information criterion was used to select among eight plausible models of chromosome evolution including combinations of constant and linear rates of dysploidization, and allowing for demi-polyploidization or whole-genome duplications (see Mayrose et al., 2010; Glick & Mayrose, 2014). Ancestral chromosome numbers were subsequently estimated under the preferred model using 1000 simulations. To test for bias in the chromosome number inferred at the root of the phylogeny caused by the earliest diverging lineage, *Galeana pratensis* ($x = 9$), we replicated the analysis with this taxon excluded, and with the coded chromosome number altered to reflect the cytogenetic variability present in unsampled members of subtribe Galeaninae (i.e., *Villanova*, $x = 20$). Data and scripts associated with the analyses described here can be found online at Dryad (Data S1).

3 Results

3.1 Genome skimming

Massively parallel sequencing of libraries derived from field and herbarium leaf tissue for genome skimming resulted in 134 Gb of raw data. Removal of samples with less than 1 000 000 reads after adapter trimming and quality filtering yielded data for 70 of 84 species in Perityleae, averaging 2.1 GB of data per sample. Reference guided assembly of whole plastomes and nuclear ribosomal cistrons, alignment with MAFFT, and removal of gappy regions yielded a data matrix of ~150 000 bp cpDNA and ~8500 bp nrDNA for 74 accessions, including multiple samples for the bi-continentally distributed *Perityle emoryi*.

Maximum likelihood and Bayesian statistical inference methods yielded equivalent topologies for cpDNA and for nrDNA, but phylogenies produced using a Bayesian approach had consistently higher support values than maximum likelihood trees. In the cpDNA tree, tribe Perityleae was not recovered as monophyletic as the only representative of subtribe Galeaninae, *Galeana pratensis*, grouped with sampled members of the Eupatorieae tribe (Figs. 2, S1, S2). Monophyly of subtribe Per4tylinae sensu Robinson (1981) was supported by cpDNA, but monophyly of the diverse genus *Perityle* was not supported (Fig. 2). Internal branches of the cpDNA phylogeny had high support (Figs. S1, S2), but relationships among genera and infrageneric sections did not agree with past taxonomic hypotheses based on morphology and chromosome numbers. *Eutetras* was resolved as nested within a clade of members of *Perityle* found in the southern Sierra Madre Occidental of Mexico and *Amauria* was resolved as highly nested within *Perityle* in the cpDNA phylogeny.

Trees based on nrDNA also did not recover Perityleae as a monophyletic group, with *Galeana pratensis* weakly resolved outside of Eupatorieae and Peritylinae, which together form a maximally supported monophyletic group (Figs. 2, 3, S3, S4). Subtribe Peritylinae was resolved as monophyletic with high support. Relationships within subtribe Peritylinae were resolved with high or moderate support in the nrDNA tree, but they conflicted extensively with the cpDNA tree in topology (Fig. 2). Members of *Perityle* were found to be paraphyletic and split between two groups, with a first group of Baja California taxa (*P. californica* Benth., *P. crassifolia* Brandegee, *P. cuneata* Brandegee, and *P. incompta* Brandegee) and the only Chilean sample of *Perityle emoryi* Torr., with $x = 11$, 12, 13, 16, and 19 chromosomes, forming a clade that is sister to *Amauria* ($x = 18$, 20), *Pericome* ($x = 18$), and the rest of genus *Perityle,* all taxa of which possess a base chromosome number of $x = 17$. The *second* clade containing all *Perityle* taxa, except those in the Baja California group mentioned above, was divided in turn into three more groups. The first is of unresolved position in the nrDNA tree and contains two historically understudied taxa, *Perityle rosei* Greenm. and *Perityle trichodonta* S.F. Blake (Figs. 2, S3, S4). The second group (e.g., *P. ciliata* Rydb., *P. hofmeisteria* Rydb., *P. jaliscana* A. Gray, and *P. microglossa* Benth.) roughly corresponds to the previously recognized white ray corolla series of *Perityle* sect. *Perityle* sensu Powell (1974) with the exclusion of *Perityle crassifolia*. The third and largest group contains all remaining members of *Perityle* sect. *Perityle* and
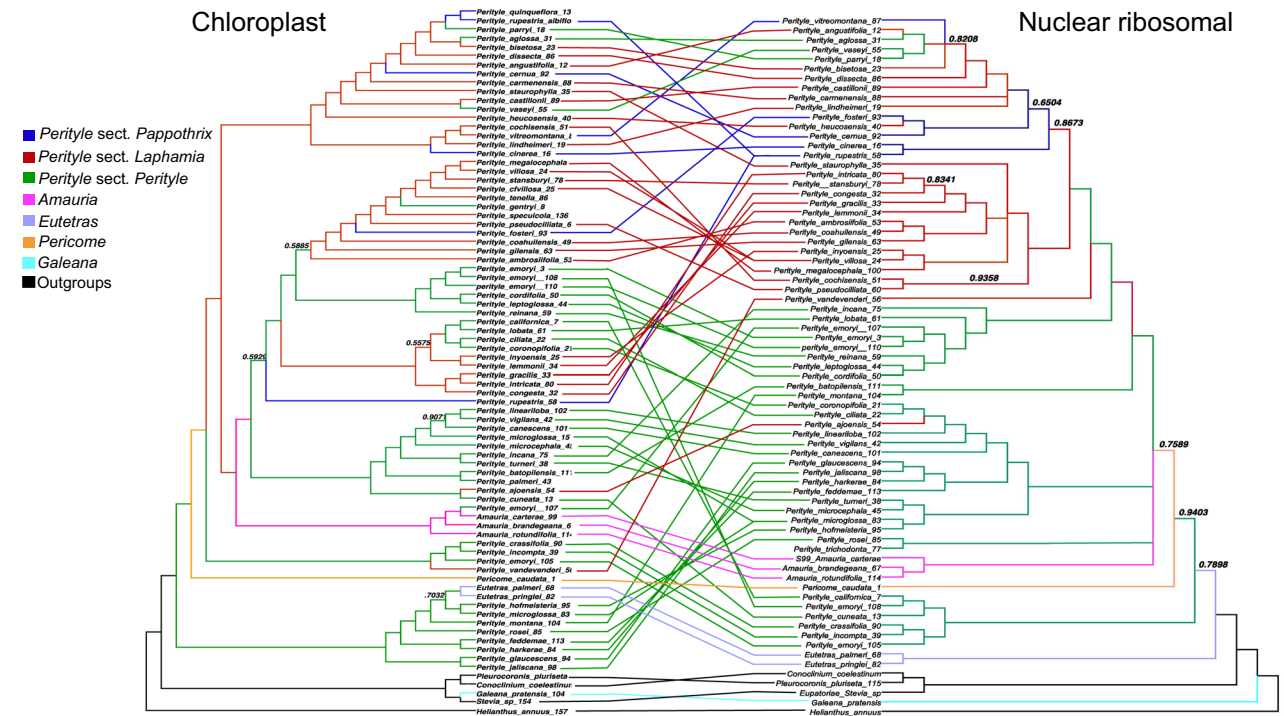
Chloroplast | Nuclear ribosomal

Fig. 2. A tanglegram of phylogenetic trees based on whole chloroplast genomes and nuclear ribosomal cistrons. Tree topologies represent the maximum a posteriori topology inferred with Markov Chain Monte Carlo (MCMC) in RevBayes (Höhna et al., 2016) conditioned on a GTR + gamma + I model of molecular substitution for 30 000 generations. Branches with less than 0.5 posterior support are collapsed and branches with less than 0.95 pp are annotated in the figure. Colors of internal lines and links between terminals indicate major taxonomic groups within Perityleae.

the entirety of *Perityle* sect. *Laphamia* and *Perityle* sect. *Pappothrix*.

3.2 Conserved orthologous sequences

Sequencing of a subset of samples enriched for hundreds of low-copy nuclear loci resulted in 142 Gb of raw sequence data. After adapter trimming and quality filtering, samples with less than 1 000 000 reads were omitted, and the data set was pared down to one sample per taxon. De novo assembly and removal of suspected paralogs resulted in an average recovery of 214 out of 1060 COS markers, with a range between 5 and 436 orthologs per sample. Exclusion of suspected paralogs resulted in a considerable loss of data for the polyploids *Perityle emoryi* and *Perityle incana* A. Gray, with 5–12 and 8 orthologous markers recovered, respectively, and these samples were excluded from further analyses. In total, 212 alignments with >50% of taxa were selected for concatenation or used in Astral analyses.

As with cpDNA and nrDNA data sets, maximum likelihood and Bayesian inference of a concatenated matrix of targeted low-copy nuclear loci produced roughly equivalent topologies, with higher branch support in Bayesian trees (Figs. S5, S6). Monophyly of Perityleae was highly supported by the low-copy nuclear data, with the only sampled member of Galeaninae, *Galeana pratensis*, resolving as sister to other sampled members of the tribe (Figs. 3, S5, S6). Within subtribe Peritylinae, the genus *Perityle* was again recovered as paraphyletic and split between three groups. First, the

clade containing the Baja California herbaceous taxa *Perityle californica*, *P. crassifolia*, and *P. cuneata* was placed with the two sampled members of *Amauria* (Fig. 3). Second, *Perityle trichodonta* S.T. Blake was resolved on its own in a clade with *Eutetras pringlei* Greenm., and *Pericome caudata* A. Gray as sister to all other members of Peritylinae, with the clade containing *Amauria*, *Perityle californica*, *P. crassifolia*, and *P. cuneata* as sister to the rest of genus *Perityle*. The third and final clade contained all remaining representatives of *Perityle* and was composed of two groups. First, a clade (e.g., with *P. ciliata* Rydb., *P. hofmeisteria* Rydb., *P. jaliscana* A. Gray, and *P. microglossa* Benth.) was resolved that corresponds roughly to the white ray corolla series of *Perityle* sect. *Perityle* sensu Powell (1974). Second is a group (e.g., with *P. cochisensis* (W.E. Niles) A.M. Powell, *P. leptoglossa* Harv. & A. Gray., *P. montana* (A.M. Powell) B.G. Baldwin, and *P. parryi* A. Gray) that includes all members of *Perityle* sect. *Laphamia* and *Perityle* sect. *Pappothrix*, as well as the yellow ray corolla series of sect. *Perityle*, with the exceptions of *Perityle californica* and *P. cuneata* (Figs. 3, 4). The ASTRAL tree was similar to that based on a concatenated matrix of low-copy nuclear loci, except for the position of several higher nested relationships (Fig. S7). Incongruences at shallow scales between the two trees include the positions of *Perityle ambrosiifolia* Greene ex A.M. Powell & Yarborough, *P. bisetosa* (Torr. ex A. Gray) Shinners, *P. gilensis* (M.E. Jones) A.F. Macbr., *P. turneri* A.M. Powell, *P. vitreomontana* Warnock, and the varieties of *P. megalocephala* (S. Watson)
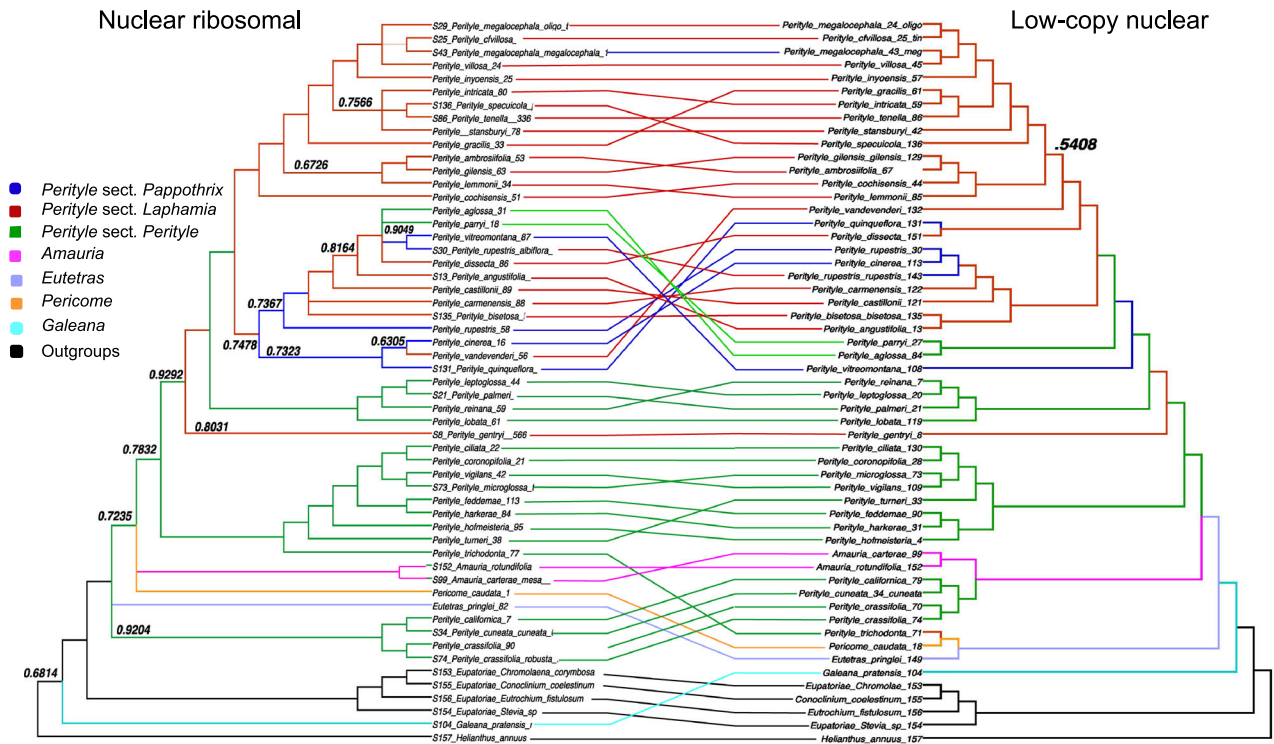
Fig. 3. A tanglegram of phylogenetic trees based on nuclear ribosomal cistrons and 212 orthologous low-copy nuclear loci. Tree topologies represent the maximum a posteriori tree topology inferred using Markov Chain Monte Carlo (MCMC) in RevBayes (Höhna et al., 2016) conditioned on a GTR + gamma + I model of molecular substitution for 30 000 generations. Branches with less than 0.5 posterior support are collapsed and branches with less than 0.95 pp are annotated in the figure. Colors of internal lines and links between terminals indicate major taxonomic groups within Perityleae.

J.F. Macbr. and *P. villosa* (S.F. Blake) Shinners. Moreover, support values were lower in the ASTRAL tree as compared with that inferred from a concatenated matrix.

Quantitative comparisons of trees using Robinson–Foulds distances suggested that the greatest incongruence was between nrDNA and cpDNA trees, followed by concatenated low-copy nuclear vs. cpDNA trees (Table 2). Nuclear ribosomal and concatenated low-copy nuclear gene trees showed an overall congruence at deep and shallow scales, with an apparent discordance in the clade wherein relationships were most weakly supported in the nrDNA tree and along the unresolved backbone of the nrDNA tree (Fig. 3). The phylogenetic analysis of combined nuclear ribosomal cistrons and low-copy nuclear loci resulted in the most inclusively sampled tree, with high or moderate support at most nodes (Fig. 4). Remaining phylogenetic uncertainty in the combined nuclear tree included the position of *Eutetras* in relation to the earliest diverging clade of *Perityle* (Fig. 4) and, at shallower taxonomic scales, some relationships within the most diverse and presumably most recently derived clade of *Perityle*. Groups resolved among paraphyletic *Perityle* were also supported in the combined tree and are illustrated in Fig. 4.

3.3 Ancestral state reconstructions

The maximum a posteriori model of morphological evolution supported by our analysis varied among morphological traits, but it was consistent between replicated analyses based on

different sources of molecular data, with the exception of loss of ray florets (Table 3, Figs. 5, S8, S9). Irreversible evolution was supported for the loss of callous fruit margins, transitions in disc corolla color from yellow to white, and the loss of ciliate fruit margins (Table 3). Multiple independent losses and at least one dramatic increase in abundance are supported for pappus bristle evolution, but rates of regaining bristles after being completely lost were not significantly non-zero (Table 3, Figs. 5, S9). Reversible evolution was supported for transitions involving fruit pappus scales, ray corolla color, and number of fruit sides (Table 3, Fig. S9). Transitions between radiate and discoid capitula were supported as reversible in our analysis of combined nrDNA and low-copy nuclear loci, but the transition from radiate to discoid was not significantly non-zero in the analysis based on cpDNA data (Table 3).

Model-averaged ancestral state reconstructions reveal more than one independent transition between states for each morphological character across the phylogeny of Perityleae (Figs. 5, S8). In the analyses based on the combined nrDNA and low-copy nuclear loci phylogeny, two independent transitions from ancestrally two-angled fruits to four-angled fruits occurred in the early diverging lineages corresponding to *Amauria* and *Eutetras*. Callous fruit margins were lost in four isolated cases, one of which occurred at or around the node that corresponds to the base of the highly nested lineage containing many members of *Perityle* sect. *Pappothrix*. Ciliate fruit margins are
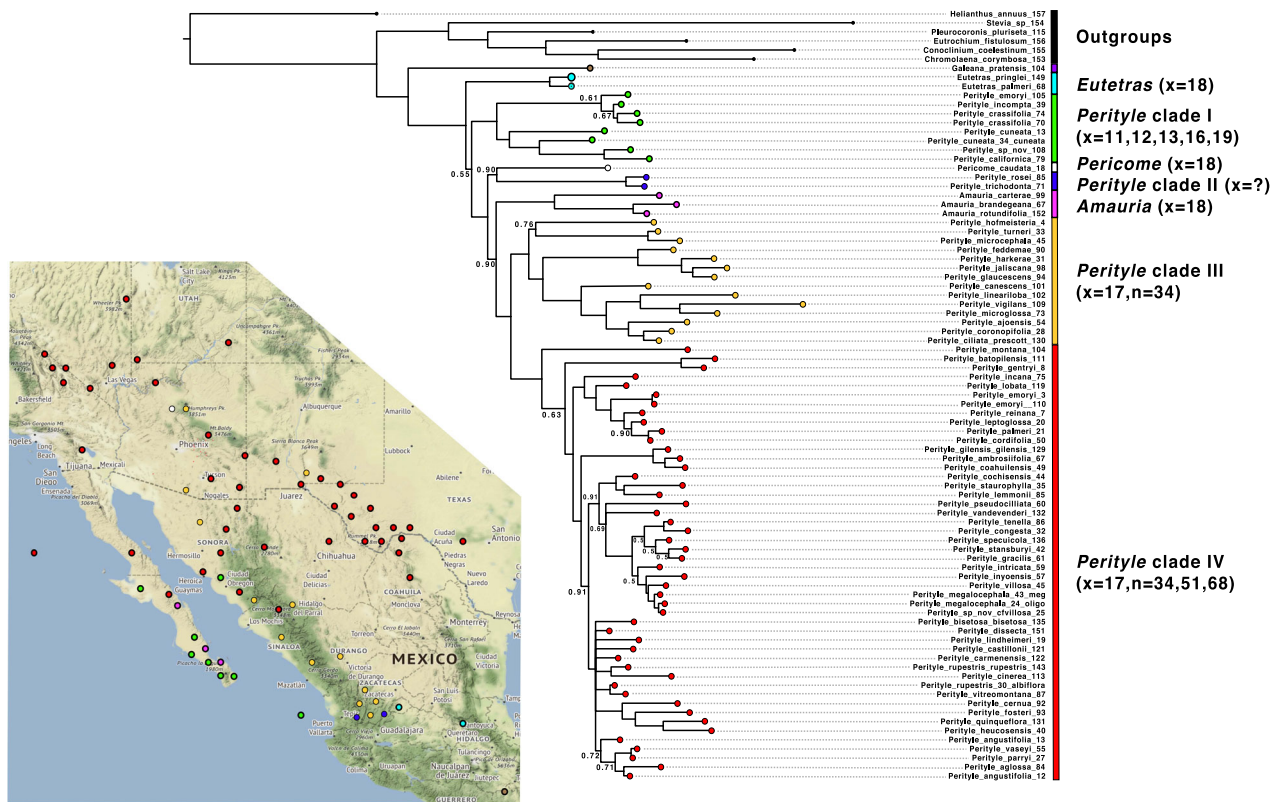
Fig. 4. The maximum a posteriori phylogenetic tree based on a combined analysis of nuclear ribosomal cistrons and orthologous low-copy nuclear loci inferred using Markov Chain Monte Carlo (MCMC) in RevBayes (Höhna et al., 2016) conditioned on an separate GTR + gamma+I model for each gene locus. MCMC was run for 30 000 generations and then inspected for stationarity and effective sample sizes greater than 500 in the software program Tracer (Rambaut et al., 2018). Branches with less than 0.5 posterior probabilities are collapsed and branches with less than 0.95 posterior probabilities are annotated. Geographical locations of the individual accessions represented at the tips are mapped, color-coded, and labeled to illustrate distributions of broad monophyletic lineages detected in this study.

supported as a dynamic characteristic gained in multiple independent cases but not readily lost. Pappus scale expression, ray corolla color, and capitulum type are all characters that underwent a transition at or around the node in the phylogeny that corresponds to *Perityle* group IV (Fig. 4); however, additional independent transitions across the phylogeny are also supported in all three cases. Pappus bristle expression shows a complicated history of multiple independent losses from an ancestral number of 1–4 bristles and one marked increase in bristle number corresponding solely to the highly nested clade that contains several members of *Perityle* sect. *Pappothrix*.

Table 2 Quantitative comparisons of relative congruence between phylogenetic trees based on whole chloroplast genomes, whole nuclear ribosomal cistrons, and 212 low-copy nuclear genes, using both a concatenated matrix and pseudo-coalescent approach in ASTRAL (Zhang et al., 2018) for a broad sample of Perityleae

Phylogenomic matrix	Phylogenomic matrix	Symmetric difference (Robinson–Foulds difference)	Branch score difference	Path difference	Quadratic path difference
Nuclear ribosomal	Chloroplast	94	0.07123977	198.29271293	1.21256784
Nuclear ribosomal	Concatenated COS UCE	58	0.7925234	133.8058295	13.4404398
Chloroplast	Concatenated COS UCE	86	0.8458701	207.9615349	14.6040614
Concatenated COS UCE	Astral COS UCE	26	N/A	65.11528	N/A

Symmetric, branch score, path, and quadratic path distances were calculated using the R package phangorn (Schliep, 2011).

Table 3 Model-averaged estimates of transition rates between morphological states obtained by reversible jump MCMC for two sources of molecular data

Molecular region	Trait	Transition	Mean transition rate	95% HPD interval	Bayes factor
nrDNA + COS	Pappus scales	Absent to present	0.1707	0.0367–0.3327	0
		Present to absent	0.164	0.185–0.5047	0
Chloroplast		Absent to present	0.4041	0–0.8811	0.01
		Present to absent	0.4142	0–0.9693	0.01
nrDNA + COS	Callous fruit margins	Absent to present	0.0191	0–0.0862	0.91*
		Present to absent	0.1376	0.0456–0.255	0
Chloroplast		Absent to present	0.0346	0–0.1661	1.020*
		Present to absent	0.5377	0.1689–0.9745	0
nrDNA + COS	Ciliate fruit margins	Absent to present	0.2626	0.1196–0.4372	0
		Present to absent	0.016	0–0.0738	0.98*
Chloroplast		Absent to present	0.8344	0.2982–1.3486	0
		Present to absent	0.0315	0–0.1535	1.17*
nrDNA + COS	Ray corolla color	White to yellow	0.092	0.0106–0.1969	0
		Yellow to white	0.0973	0,0.2131	0
Chloroplast		White to yellow	0.2261	0–1.096	0.32
		Yellow to white	0.2758	0–1.0832	0.32
nrDNA + COS	Disc corolla color	White to yellow	0.0196	0–0.0912	1.06*
		Yellow to white	0.1903	0.0736–0.3111	0
Chloroplast		White to yellow	0.0296	0–01391	0.98*
		Yellow to white	0.3332	0.0902–0.6617	0
nrDNA + COS	Number of fruit sides	4 to 2	0.0181	0–0.0835	1
		2 to 4	0.0887	0.008–0.1932	0
Chloroplast		4 to 2			0.05
		2 to 4			0
nrDNA + COS	Capitula	Discoid to radiate	0.2305	0.0797–0.4008	0
		Radiate to discoid	0.1935	0.0711–0.3245	0
Chloroplast		Discoid to radiate	0.6741	0.1812–1.4649	0
		Radiate to discoid	0.0173	0–0.0874	1.2*
nrDNA + COS	Pappus bristles	0 to 1–4	0.553	0–2.5559	0.86
		0 to 10–35	0.425	0–2.1185	1.23*
		1–4 to 0	7.239	1.6222–14.3219	0
		1–4 to 10–35	1.201	0–3.2656	0.01
		10–35 to 0	0.477	0–2.3309	1.18*
		10–35 to 1–4	0.58	0–2.5899	0.85
Chloroplast	Pappus bristles	0 to 1–4	3.908	0–0.1691	0.74
		0 to 10–35	2.622	0–0.1273	1.140*
		1–4 to 0	0.43	0.1303–0.8356	0
		1–4 to 10–35	0.222	0.096–0.4752	0
		10–35 to 0	2.658	0–0.1295	1.14*
		10–35 to 1–4	2.932	0–0.1348	0.92*

Mean transition rates are reported as changes per unit branch length with HPD confidence intervals of 95%. The evidence for reversible morphological evolution was assessed using Bayes factors, with values greater than 0.90 suggesting strong support for irreversibility and values less than 0.1 suggesting strong support for reversibility. Significant Bayes factors are indicated with a *.
COS, conserved ortholog set; HPD, highest posterior density; MCMC, Markov Chain Monte Carlo; nrDNA, nuclear ribosomal DNA.

3.4 Chromosome evolution

Model testing with AIC supports the use of a model of chromosome evolution that includes rates for dysploid gains or losses, demi-polyploidy, and polyploidization that are independent of the current chromosome number (Table 4). The same model was supported for trees based on both genomic sources of molecular data (Table 4). Reconstruction of ancestral chromosome numbers on the combined nrDNA and low-copy nuclear tree (Fig. 5) suggests a base chromosome number of $x = 9$ for tribe Perityleae. Two independent polyploid events, one dysploid increase, and one demi-polyploidization event are supported as giving rise to the varied chromosome numbers of the earliest diverging lineages of tribe Perityleae, which include $x = 11$, 12, 16, 18, and 19. For the majority of Perityleae, polyploidization followed by a dysploid loss of one chromosome resulted in a stabilized ancestral chromosome number of $x = 17$ that was resolved for all internal nodes of Perityle clades III and IV (Figs. 4, 5).
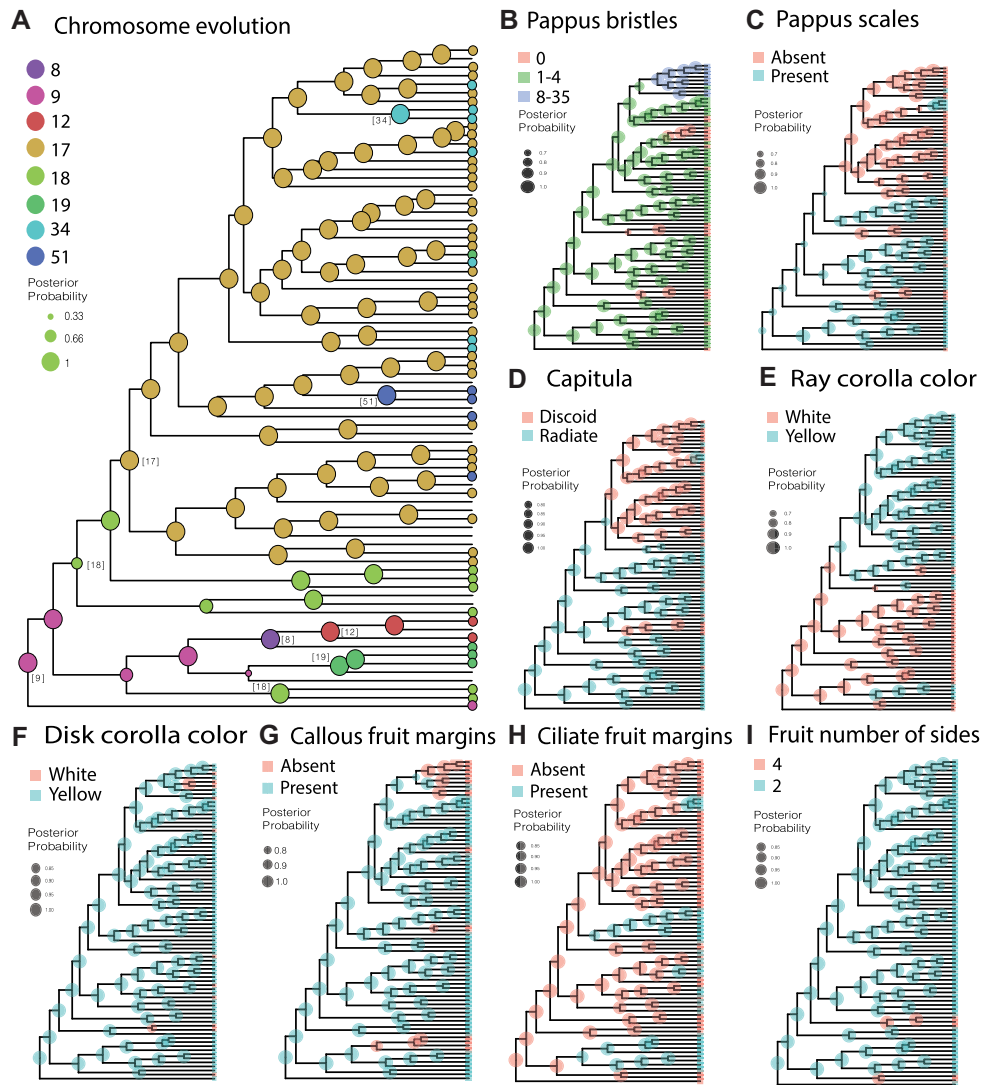
Fig. 5. Maximum likelihood reconstruction of ancestral chromosome numbers (**A**) and model-averaged maximum a posteriori ancestral state reconstructions (**B–I**) of morphological traits traditionally emphasized in Perityleae classification. **A,** Ancestral chromosome numbers were reconstructed under the CONST_RATE_DEMI_EST model in the software program ChromEvol (Mayrose et al., 2010; Glick & Mayrose, 2014) on the map phylogenetic tree based on combined nrDNA and low-copy nuclear loci. Tips that are missing color-coded labels are of unknown chromosome number. **B–I,** Maximum a posteriori ancestral state reconstructions were compiled from a posterior distribution of 1200 stochastic character maps generated using reversible jump MCMC in RevBayes (Höhna et al., 2016). Stochastic character maps were conditioned on two plausible models for each transition rate, either a reversible (non-zero) or an irreversible (zero) rate, and mapped on a posterior distribution of 604 trees generated by our Bayesian inference of tree topology based on combined nrDNA and low-copy nuclear loci.

Neopolyploidy is also suggested to be an important process giving rise to cytogenetic variation at shallower scales throughout the $x = 17$ clade, which includes polyploid taxa with $2n = 34$, 51, and 68 pairs. Replicating analyses with *Galeana pratensis* ($x = 9$) recoded to represent variability in Galeaninae ($x = 9$, 20) did not lead to differences in the reconstructed root chromosome number or inferred transitions in chromosome number. Removal of *Galeana pratensis* from the analysis resulted in an estimated root chromosome number of $x = 12$ for subtribe Peritylinae, with one demi-polyploidization and dysploid increase giving rise to the contemporary variation in the earliest diverging lineages of Perityleae (Fig. S10).

4 Discussion

4.1 General performance of phylogenomic approaches in Perityleae

The phylogenomic approaches used in this study differed in terms of their sampling capacity, inferred statistical support, and degree of discordance with other lines of evidence. Sampling Perityleae for molecular analysis is challenging, because it is a diverse group found in hard-to-reach environments and known from few collections. The genome skimming approach was successful with old and degraded herbarium specimens, making it possible to densely sample

Table 4 Likelihood estimates of alternative models of chromosome evolution available in the maximum likelihood-based software program ChromEvol (Glick & Mayrose, 2014)

Source of molecular data	Model of chromosome evolution	Log-likelihood	AIC
nrDNA + COS loci	Constant rate	−109	224.1
	Constant rate with demi-polyploidization	−76.2	158.4
	Constant rate with demi-polyploidization + ETA	−75.08	158.2
	Constant rate with no polyploidization	−247.5	499
	Linear rate	108.7	227.4
	Linear rate with demi-polyploidization	−76.08	162.2
	Linear rate with demi-polyploidization + EST	−74.96	161.9
	Linear rate with no polyploidization	−212.9	433.8
Chloroplast genome	Constant rate	−154.4	314.9
	Constant rate with demi-polyploidization	−113.4	232.8
	Constant rate with demi-polyploidization + ETA	−111.7	231.5
	Constant rate with no polyploidization	−266.2	536.5
	Linear rate	−154.7	319.4
	Linear rate with demi-polyploidization	−113.1	236.2
	Linear rate with demi-polyploidization + EST	−112.2	236.4
	Linear rate with no polyploidization	−223.8	455.6

Log-likelihood and Akaike Information Criteria were used in model testing for two independent molecular sources of data. More information about the models implemented here can be found in Mayrose et al. (2010) and Glick & Mayrose (2014). AIC, akaike information criterion; COS, conserved ortholog set; nrDNA, nuclear ribosomal DNA.

Perityleae for plastomes and nuclear ribosomal regions. Target capture of low-copy nuclear data was limited to a subset of taxa wherein DNA extracts of sufficiently high concentration and quality could be obtained. Support for relationships was strong in the trees based on chloroplast genomes and low-copy nuclear loci, and generally intermediate (but often not at the deepest or finest taxonomic scales) in the nrDNA tree. Both the low-copy nuclear and nrDNA trees resolved a similar subset of monophyletic groups within Perityleae, with topological incongruence mostly involving the clade wherein support values were low in the nrDNA tree (Fig. 3). The cpDNA tree showed the greatest discordance with each of the other sources of data (Table 2), with rampant incongruence evident both across and within genera (Fig. 2). The phylogenetic analysis of combined nrDNA and low-copy nuclear loci produced the most densely sampled and well-resolved phylogenetic hypothesis of Perityleae to date, but the future addition of difficult-to-obtain taxa and expanded sampling within species should refine this hypothesis.

Published applications of the Compositae COS loci to various tribes and genera has accelerated since the publication of this unique set of baits became publicly available. This target-capture method has been used empirically to study the backbone of the family (Mandel et al., 2019; Watson et al., 2020) and the large tribes Vernonieae Cass. (Siniscalchi et al., 2019) and Cardueae Cass (Herrando-Moraira et al., 2019). Recently, the bait set has been tested at varying taxonomic levels (Jones et al., 2019) and applied within genera in *Cirsium* Mill. (Ackerfield J, pers. comm.) and *Antennaria* Gaertn. (Thapa et al., 2020). In the present study, the first using target capture to densely sample a tribe within the Heliantheae alliance, the method yielded phylogenetic trees with strong statistical support. By far the greatest loss of data occurred while filtering gene regions suspected of paralogy, which amounted to an

average of 846 of 1060 gene regions per sample. As reported in Thapa et al. (2020), it was necessary to exclude polyploid taxa, in particular *Perityle emoryi* and *P. incana,* because all but as few as five gene regions in some cases were flagged and eliminated as paralogs. Close to a third of taxa of *Perityle* are polyploids, but at present the autopolyploids cannot be discerned from allopolyploids. Although *P. emoryi* and *P. incana* were not the only polyploids included in this study, they were the only ones with such a large number of suspected paralogs, suggesting that they may have allopolyploid origins. It is concerning that an average of >75% of the low-copy nuclear gene regions sequenced were discarded because of paralogy, but this result is also not unexpected. Perityleae occupies a highly nested position within the Compositae, wherein a history of whole-genome duplication and parallel retention of duplicate genes is likely to contribute to widespread paralogy (Barker et al., 2008). Improved bioinformatic procedures that effectively separate and subset or phase paralogous gene regions (Gardner et al., 2019; Freyman et al., 2020), rather than excluding them, could be useful both for increasing statistical support as well as understanding the hybrid origins of putatively allopolyploid taxa (e.g., Brandrud et al., 2020).

4.2 Extent and sources of phylogenetic incongruence in Perityleae

The promise of phylogenomics to overcome obstacles of limited sampling and poor statistical support should be tempered with the understanding that more sequence data will reveal more discordances between genetic lines of evidence (Sayyari et al., 2018). Species tree discordance may be due to phylogenetic uncertainty, ILS, or hybridization (Rieseberg & Soltis, 1991; Maddison, 1997; Huelsenbeck et al., 2000). In this study, phylogenetic uncertainty was present in the nrDNA tree and likely contributed to incongruence between this tree and the trees based on low-copy nuclear

loci. The extensive incongruence seen between the well-supported cpDNA tree and all nuclear DNA trees, however, was likely due to ILS and introgression or hybridization. With a few exceptions, hybridization has not previously been viewed as an important evolutionary process in Perityleae due to the strictly allopatric distribution of most taxa (Powell, 1974). However, even among geographically separated populations, sporadic contact can lead to chloroplast capture via introgressive hybridization (Rieseberg & Soltis, 1991). Although we did not explicitly reconstruct geographic dispersal, incongruence between cpDNA and nuclear DNA trees does indicate a secondary contact between previously geographically isolated lineages in some cases. For example, *Perityle lobata* (Rydb.) I.M. Johnst. is found in Baja California, Mexico, and was resolved as sister to *Perityle californica,* also in Baja California, in the chloroplast tree (Fig. 2). In the low-copy nuclear and nrDNA tree, however, *P. lobata* is nested within a group of taxa from Sonora, Mexico, that share similar morphology and the same base chromosome number (Figs. 3, S6). On the basis of these data, it appears likely that a chloroplast capture event occurred after dispersal of *P. lobata* from mainland Mexico to the Baja California peninsula. Powell (1970) described a naturally occurring hybrid *Perityle* in southwest Texas, but efforts to relocate hybrids at that locality have been unsuccessful, suggesting that it resulted from a sporadic phenomenon. Hybridization is an important factor for the rapid diversification of recently derived plant groups (Barrier et al., 1999; Meier et al., 2017; Vargas et al., 2017). Future study is warranted to determine the prevalence of reticulation in Perityleae in further detail and to understand the impact hybridization has had on diversification of the tribe.

A comparison of the COS marker trees inferred from a total concatenated matrix (Fig. S5) versus separate gene trees while accounting for gene tree discordance (ASTRAL, Fig. S6) reveals the prevalence of ILS. Notably, the trees disagree about the placement of two early diverging lineages in Perityleae. The concatenated tree places the clade containing *Eutetras pringlei, Pericome caudata,* and *Perityle trichodonta* as sister to the rest of subtribe Peritylinae. The ASTRAL tree, however, places the clade with *Amauria carterae, A. rotundifolia, Perityle californica, P. crassifolia,* and *P. cuneata* as the earliest diverging lineage of the subtribe. The topologies of many apical relationships are reconstructed differently by the two approaches, and, furthermore, support values were lower in the ASTRAL tree in areas of similar topology. These results suggest that hybridization is unlikely to be the sole process contributing to incongruence between Perityleae species trees and gene trees; ILS and introgressive hybridization likely work in tandem to generate Perityleae gene tree incongruence. Most taxa in Perityleae are reproductively self-incompatible (Powell, 1972c) shrubs or subshrubs rooted in rock cliffs (Powell, 1968a, 1973a, 1974). Although generation-time estimates for shrubby Perityleae are not available, observations of minimal growth in individuals of *Perityle lemmonii* (A. Gray) J.F. Macbr. over 30 years in Finger Rock Canyon, Arizona, suggest that growth rates may be very slow in Perityleae (Bertelsen, 2018). Plants of rock cliffs have been found to grow more slowly in general and reach an older

maximum age on the low-quality soils of rock cliff exposures as compared with surrounding high-quality soils (Larson et al., 2005; Hopper, 2009). Long generation times, reproductive traits, and whole-genome duplications will exacerbate the effects of ILS by extending the time to coalescence (Maddison, 1997). Considering this, a multiple species coalescent approach (Heled & Drummond, 2009) should form an important part of future studies of Perityleae and other composites that share similar reproductive, life history, or genomic quirks. Denser sampling of *Eutetras, Pericome,* and *Amauria* and phylogenetic analysis in a fully implemented multiple coalescent framework should be helpful for achieving a more refined understanding of deeper generic relationships in Perityleae.

4.3 Systematic implications of phylogenomic findings
On the basis of low-copy nuclear data, the tribe Perityleae is supported as monophyletic, with the only sampled member of subtribe Galeaninae, *Galeana pratensis,* resolved as the sister group to the rest of the tribe (Fig. 4). The genera *Galeana* La Llave and *Villanova* Lag. constitute the "Villanova clade," whose position has been viewed as *incertae sedis* in the past (Baldwin et al., 2002). Panero (2007) placed Galeaninae within Perityleae on the basis of cpDNA, in agreement with the low-copy nuclear findings for *Galeana,* despite the fact that they lack the four-lobed corollas characteristic of the rest of the tribe. The plastome tree in the present study resolved *Galeana pratensis* as more closely related to members of tribe Eupatorieae than Perityleae (Fig. 2). The earlier inconclusive position of the "Villanova clade" based on ITS data (Baldwin et al., 2002) also holds for our nrDNA tree (Fig. 2), where *Galeana pratensis* was resolved as sister to Eupatorieae and Perityleae with poor (<0.5) bootstrap support. Expanded sampling of the two genera and ~12 species of the Villanova clade in a broader context of Heliantheae s.l. is warranted to clarify the evolutionary relationships of this enigmatic group.

Dense taxon sampling of Peritylinae supports the mono-phyly of this subtribe, which has long been recognized as a natural group within the Heliantheae s.l. on the basis of a four-lobed disc corolla (Rydberg, 1914; Powell & Turner, 1974: Robinson, 1981). This trait is rare in the Heliantheae alliance, but it is exhibited by *Iltisia* S.F. Blake (Eupatorieae), *Holoschkuhria* H. Rob. (Bahieae B.G. Baldwin), and subtribe Lycapsinae of Perityleae (Robinson, 1981), which was not sampled in this study. The genus *Perityle,* which contains the majority of taxa in Peritylinae (~66 spp.), was not resolved as monophyletic in any of the phylogenomic analyses conducted in this study. Circumscription of *Perityle* has been in flux since the original generic circumscription by Bentham (1844, p. 23) based on the type species, *Perityle californica,* an annual of decomposed substrates (soil and gravel) in the Sonoran Desert. *Laphamia* was described by Asa Gray (1852) to accommodate subshrubby species rooted in rock cliffs that seemed to represent an opposing morphological extreme; however, morphological grounds for separating *Laphamia* from *Perityle* became complicated when new, intermediate species were described. The challenge for subsequent authors was to determine the traits that had to be focused upon and the method of weighing the taxonomic significance of various polymorphic fruit and

flower traits. Thus, Rydberg (1914) split five additional genera from *Perityle* and *Laphamia* based on minute differences in pappus morphology. Everly (1947) reorganized these into *Perityle*, *Laphamia*, and *Pappothrix*. The present circumscription results from Shinner's (1959) lumping of *Laphamia* and *Pappothrix* into *Perityle*, based on the view that pappus morphology was too labile for delimiting genera. Powell (1968a), author of the most recent comprehensive treatment of *Perityle* (Powell, 1973a, 1974), upheld Shinner's inclusive generic concept, but retained *Perityle*, *Laphamia*, and *Pappothrix* as infrageneric sections. In nrDNA and low-copy nuclear gene trees, *Perityle* was resolved as paraphyletic (Figs. 3, 4), with a subset of species of *Perityle* sect. *Perityle* resolved as more closely related to *Amauria* than to other members of *Perityle*. This latter group contains the type species of *Perityle*, *P. californica*, as well as *P. crassifolia* and *P. cuneata* (*Perityle* clade I, Fig. 4). These taxa were singled out by Powell in the past for being anomalous in the genus *Perityle* due to their annual life history, occurrence in gravel and soil rather than rock cliffs, and unique chromosome numbers, including $x = 11, 12, 13, 16$, and 19 (Powell, 1974). A second *Perityle* clade (*Perityle* clade II, Fig. 4) is resolved as sister to *Pericome caudata* and composed of *Perityle rosei* and *Perityle trichodonta*, two narrow endemics to the southern portion of the Sierra Madre Occidental in Mexico, with chromosome numbers that remain unknown. All other taxa in *Perityle* (Perityle clades III and IV, Fig. 4) are resolved as a large clade in nrDNA and low-copy nuclear gene trees and have a base chromosome number of $x = 17$ or multiples thereof ($n = 34, 51, 68$).

In phylogenetic trees based on nrDNA and low-copy nuclear loci, *Perityle* sect. *Perityle*, *Perityle* sect. *Laphamia*, and *Perityle* sect. *Pappothrix* represent a non-monophyletic assemblage of taxa (Fig. 3). Members of *Perityle* sect. *Perityle* are distributed among four separate clades (Fig. 3). The earliest diverging lineage is the group mentioned above that contains the type species of *Perityle*, *P. californica*, and is more closely related to *Amauria* than to other members of *Perityle*. Within the clade that contains the rest of *Perityle* (*Perityle* clades III and IV, Fig. 4), the earliest diverging lineage is a clade of perennial and annual herbs of *Perityle* sect. *Perityle* that possess white ray corollas or no ray florets (Figs. 3, 4). These taxa roughly correspond to a natural group described by Powell as the white ray corolla series, which is distributed throughout the Sierra Madre Occidental in northwest Mexico and into the sky islands of Arizona and New Mexico (Powell, 1974). The third group of *Perityle* sect. *Perityle* contains most members of Powell's yellow ray corolla series (Powell, 1974) and forms a basal grade to *Perityle* sect. *Laphamia* in the nrDNA and low-copy nuclear trees (Figs. 3, 4). In the nrDNA tree, this third group also includes the polyploids *Perityle emoryi*, a widespread annual with white ray corollas, and *Perityle incana*, a discoid-headed shrub endemic to Guadalupe Island, Mexico (Figs. 3, 4). These two taxa were excluded from analyses using solely the low-copy nuclear data set due to data loss during filtering of suspected paralogs. In the cpDNA tree (Fig. 2), three samples of *P. emoryi* are placed in this same clade, but the fourth is nested within *Amauria*, and *P. incana* is placed within the white ray corolla series. These incongruences support the hypothesized allopolyploid origins of *P. emoryi* and *P. incana*,

as discussed above. The fourth group of *Perityle* sect. *Perityle* includes *P. aglossa* A. Gray, *P. parryi* A. Gray, and *P. vaseyi* J.M. Coult. (in nrDNA data), which form a highly nested clade within *Perityle* sect. *Laphamia* (Fig. 3). These taxa were also viewed as anomalous by Powell, because they share morphological affinities with the yellow ray corolla series but are geographically disjunct from the rest of that group in southwest Texas and northern Chihuahua, Mexico (Powell, 1974).

Both *Perityle* sect. *Laphamia* and *Perityle* sect. *Pappothrix* consist entirely of species of subshrubs that grow on rocky cliffs in mountains and canyons of the northern Sonoran, Chihuahuan, and Great Basin deserts (Powell, 1969, 1973a). *Perityle* sect. *Pappothrix* contains seven taxa, all five of which that were sampled in this study were nested within *Perityle* sect. *Laphamia* in all three phylogenomic analyses. If *Perityle* sect. *Pappothrix* is treated as a synonym of *Perityle* sect. *Laphamia*, then *Perityle* sect. *Laphamia* represents a natural group with the exception of *Perityle gentryi* A.M. Powell (Fig. 3). *Perityle gentryi* has long been considered an outlier in *Perityle* sect. *Laphamia*, because it is geographically disjunct in western Sonora and Sinaloa, Mexico, where it grows on rocky outcrops in tropical deciduous forest (TDF) habitats (Powell, 1973a). *Perityle batopilensis* A.M. Powell and *Perityle montana* (A.M. Powell) B.G. Baldwin, also in TDF in northwest Mexico, form a clade with *P. gentryi* in the nrDNA tree and with weak support in the combined nuclear analysis as well (Figs. 3, 4). Two unsampled species, *Perityle grandifolia* and *P. lloydii* B.L. Rob. & Fernald, are morphologically similar to *P. gentryi* and also found in TDF, and therefore may belong to this previously undetected clade, which is in need of more study. There exist two subclades within the group that contains the rest of *Perityle* sect. *Laphamia* and all of *Perityle* sect. *Pappothrix* (Figs. 3, 4). One clade contains mostly members of *Perityle* sect. *Laphamia* and corresponds to the group informally named by Powell as the "southwestern alliance" (Powell, 1973a, Fig. 4). These include discoid-headed, perennial subshrubs rooted in limestone and volcanic cliffs in Arizona, California, Nevada, and Utah. Several taxa viewed by Powell as anomalous resolve as part of the southwestern alliance in the nrDNA and low-copy nuclear trees, including *Perityle cochisensis* (W.E. Niles) A.M. Powell, *P. lemmonii*, *P. stansburyi* (A. Gray) J.F. Macbr., and *P. vandevenderi* B.L. Turner (Powell, 1973a, Fig. 4). In the low-copy nuclear tree, members of *Perityle* sect. *Pappothrix* are resolved as a polyphyletic assemblage nested within a grade of taxa from *Perityle* sect. *Laphamia*. The combined analysis of nrDNA and low-copy nuclear loci resolved the extant members of *Perityle* sect. *Pappothrix* within a clade with *Perityle lindheimeri* but with poor support. The taxa that constitute *Perityle* sect. *Pappothrix*, which are in need of further study, are all subshrubs rooted in rocky cliffs that occur as narrow geographic or edaphic endemics in the Chihuahuan Desert of New Mexico and Texas, United States, and Chihuahua and Coahuila, Mexico.

4.4 Evolutionary lability of morphological characters emphasized in previous taxonomies
Our results suggest that morphological characters traditionally used to classify members of Perityleae have evolved multiple times within the group (Figs. 5, S9, Table 3) and

show more lability than previously believed. Cypselae in Perityleae can be two- or four-angled in cross-section, and this has long been one of the principal characters for broadly classifying genera in this group. Four-angled fruits are present in *Amauria*, with three species found in Baja California Sur, and *Eutetras,* with two species found in the bajillo region of central Mexico. Ancestral state reconstructions suggest that four-angled fruits evolved independently in these two lineages from ancestors with two-angled fruits.

Pappus elements have been particularly emphasized in classification of Perityleae and even seen as diagnostic at the generic rank in some cases, yet our data supports Shinners' (1959) view that callous or ciliate fruit margins and pappus scales or bristles are dynamic traits that have been lost or gained in multiple independent instances. We found that callous fruit margins are ancestral and present in most extant Perityleae, but that they have been lost in a few independent and isolated instances. Ciliate fruit margins were ancestrally absent in the group, but long ciliate hairs have evolved multiple times and never been lost. The common ancestor of Perityleae is reconstructed in our study as possessing fruits with both bristles and a crown of scales. Pappus scales have had a dynamic history in Perityleae, having been lost at several deeper nodes in the phylogeny and then regained at shallower timescales. The maximally supported model of pappus bristle evolution was the one in which transitions from zero bristles to 1 to 4 or 10 to 35 bristles were not allowed, meaning that bristles were lost, but never regained after being completely lost throughout the evolutionary history of Perityleae. The complete loss of bristles occurred in many independent instances; however, in one case, there was a dramatic increase in number of bristles from one to four to as many as 35. These results suggesting a dynamic evolutionary history of pappus elements agree with studies using micro-characters (Robinson, 1981) and molecular data (Baldwin et al., 2002) that have suggested more generally that pappus elements have been overemphasized in taxonomic study of the Heliantheae alliance.

Although their importance has been weighed differently by various authors, presence or number of pappus bristles has been one of the most important characters in the classification of Perityleae (Everly, 1947; Shinners, 1959; Niles, 1970; Powell, 1969, 1973a, 1974). At the same time, ecological studies of seed dispersal suggest that pappus elements may be under intense selection, especially in island or island-like habitats, which could explain their observed evolutionary lability in our study group. Most taxa of Perityleae are ecological specialists on sheer rock faces of granite, volcanic, or limestone substrates in deserts. Suitable Perityleae habitats include imposing and often iconic landmarks that are geographically separated by expanses of low, hot, and dry desert. Corky, papery, or long ciliate fruit margins, as well as pappus scales and bristles may provide an essential fruit-dispersal advantage for extended wind scattering (anemochory) or attachment to birds (epizoochory). Only anecdotal observations of fruit dispersal in Perityleae are available, but dissemination on the plumage of cliff-dwelling insectivorous or migratory granivorous birds such as swallows (Hirundinidae), tyrant flycathers (Tyrannidae), and finches (Fringillidae) could explain the seemingly improbable dispersal of some taxa on far-flung rock habitats, oceanic islands, and the

South American continent in one case. However, increased dispersal may be perilous in other cases. Plants specialized to grow on specific edaphic substrates may invest heavily in defensive and desiccation tolerance traits that make them ineffective competitors off of their preferred substrate (Fine et al., 2004, 2006; Hopper, 2009; Strauss & Cacho, 2013; Cacho & Strauss, 2014; Rajakaruna, 2018). Individuals of typically rock-dwelling Perityleae that disperse off from cliff faces are rarely found surviving to maturity. The frequent and independent reductions in pappus scales and bristles suggested by our data may reflect intense selection against dispersability in these highly specialized and isolated cliff-dwelling plants. Although Perityleae may be an excellent candidate system to test hypotheses about dispersal ecology, a cautionary note is necessary before interpreting losses of pappus elements as evidence of decreased dispersability due to island effects. The loss of fruit structures could also be correlated with selection for survival in an arid climate, leading to overall reductions in fruit mass and ornaments or alternative modes of dispersal (i.e., wind versus wildlife) (Burns, 2018).

Our results suggest that characters of the capitula such as the presence of ray florets and corolla color have also transitioned multiple independent times over the history of Perityleae. Model-averaged ancestral states of ray corolla color show a transition from white to yellow ray corollas at the node leading to most members of *Perityle* clade IV (Figs. 4, 5), with other taxa having yellow ray corollas in the earliest diverging clade of *Perityle* and at least one reversal to white ray corollas in the widespread annual species *Perityle emoryi*. A loss of ray florets is likewise resolved at the node containing all highly nested members of *Perityle* clade IV; however, ray florets have been regained within this clade on multiple occasions, as well as lost in earlier diverging lineages. Our reconstruction of disc corolla color shows multiple independent transitions from ancestrally yellow to white color, but not back again. In contrast to ray corolla color and the radiate condition, which were resolved as reversible traits, transitions in disc corolla color were significantly irreversible (Table 3, Fig. S9). Ancestral reconstructions of capitula characteristics in Perityleae deserve special attention due to its sister relationship to Eupatorieae, a principally tropical tribe that is structurally dissimilar to Perityleae in possessing 5-merous disc florets, having no ray florets, lacking yellow-pigmented disc corollas, as well as having graduated involucres and well-developed style branch appendages (Robinson et al., 2007). Our results support a radiate common ancestor of Perityleae with white ray corollas and yellow disc corollas. In addition, all extant members of Perityleae have involucres of one or two series of phyllaries and unexpanded style branch appendages. An approximately 25-fold increase in species diversity in Eupatorieae (~2500 spp.) as compared with Perityleae (84 currently recognized spp.) may reflect the historical confluence of these key differences in floral morphology with the biogeographic dispersion of Eupatorieae in tropical habitats (Baldwin, 2009).

4.5 Chromosome evolution and diversification in Perityleae
Our results suggest that the best model of karyological evolution in Perityleae was one in which polyploidy and

dysploid chromosome gains and losses have occurred at a constant rate independent of current chromosome number (Table 4). These mechanisms of chromosome number change were the same processes pointed to by Robinson et al. (1981) in their broad study of chromosome number variation in the Heliantheae alliance as well as by Powell (1974) in his treatment of the cytogenetically complex *Perityle* sect. *Perityle*. The ancestral chromosome number estimation of $x = 9$ for subtribe Peritylinae also agrees with historical hypotheses about base chromosome numbers in Compositae, but it is roughly half that of the $x = 17$, 18, and 19 proposed for Heliantheae s.l. (Powell, 1974; Robinson et al., 1981). Reconstructions of base chromosome number were sensitive to the inclusion of *Galeana pratensis* ($x = 9$) as the earliest diverging lineage, with a base chromosome number of $x = 12$ estimated in its absence. Given potential bias introduced by fragmentary sampling of taxa outside Peritylinae in this case, future analyses would benefit from broader inclusion of outgroup taxa, including a broad sample of related tribes where chromosome numbers of $x = 17$ or 18 are present. A stabilized base chromosome number of $x = 17$ was consistently reconstructed at all internal nodes for *Perityle* clades III and IV (Figs. 4, 5). Polyploid chromosome numbers based on $x = 17$ of $n = 34$, 51, and 68 occur along terminal branches, mirroring the case in Heliantheae s.s. wherein strictly terminal genome duplications have been interpreted as evidence for lower diversification rates in polyploids (Mayrose et al., 2010). Species with restricted distributions upon specific geological features are common in the $x = 17$ clade of Perityleae. Although these narrow endemics themselves are not all polyploids, polyploidy may have played a role in their evolution by contributing to reproductive isolation and genomic variation. Broader sampling of Perityleae, coupled with phylogenetic comparative models of chromosome number change that incorporate diversification (Freyman & Höhna, 2018), could clarify the role of polyploidy in the evolution of Perityleae in a way that could contribute to longstanding interest in this topic in the Heliantheae alliance in general.

4.6 Concluding remarks

In light of these first phylogenomic findings for Perityleae, a significant rethinking of evolutionary relationships in the tribe, as well as the morphological and cytological traits previously used in its classification, is warranted. The tremendous amount of data now available through next-generation sequencing approaches makes it increasingly possible to resolve what would otherwise be murky relationships in this group, but more information does not necessarily mean less discordance to address between different sources of phylogenetic evidence. Still, these results are in line with familiar findings from other molecular studies in the Heliantheae alliance, including the prevalence of cytonuclear incongruence and polyploidy, the historical overemphasis of fruit traits for taxonomy, and the independent support provided by chromosome numbers for deep divergences and natural groups (Baldwin, 1997; Baldwin et al., 2002). A refined understanding of evolutionary relationships in Perityleae opens the door to taxonomic revision and more detailed studies of diversification of the tribe across the extraordinary mosaic of habitats in western North America.

The natural history of Perityleae, including adaptations of these plants to the extreme conditions of desert cliff faces, makes this tribe an excellent group for addressing questions about edaphic specialization and evolution in arid climates.

Acknowledgements

Conflict of Interest

Authors on the manuscript declare no conflict of interest.

References

Anderberg AA, Baldwin BG, Bayer RG, Breitwieser J, Jeffrey C, Dillon MO, Eldenäs P, Funk V, Garcia-Jacas N, Hind DJ, Karis PO, Lack HW, Nesom G, Nordenstam B, Oberprieler C, Panero JL, Puttock C, Robinson H, Stuessy TF, Susanna A, Urtubey E, Vogt R, Ward J, Watson LE. 2007. Compositae. In: Kadereit JW, Jeffrey C eds. *Flowering plants. Eudicots. The families and genera of vascular plants.* Berlin, Heidelberg: Springer. 8: 61–588.

Baldwin BG. 1997. Adaptive radiation of the Hawaiian silversword alliance: Congruence and conflict of phylogenetic evidence from molecular and non-molecular investigations. In: Givnish TJ, Sytsma KJ eds. *Molecular evolution and adaptive radiation.* Cambridge: Cambridge University Press. 103–128.

Baldwin BG. 2009. Heliantheae alliance. In: Funk VA, Susanna A, Stuessy TF, Bayer RJ eds. *Systematics, evolution, and biogeography of Compositae.* Vienna: International Association for Plant Taxonomy, Institute of Botany, University of Vienna. 689–711.

Baldwin BG, Kyhos DW, Dvorak J, Carr GD. 1991. Chloroplast DNA evidence for a North American origin of the Hawaiian silversword alliance (Asteraceae). *Proceedings of the National Academy of Sciences of the United States of America* 88: 1840–1843.

Baldwin BG, Wessa BL, Panero JL. 2002. Nuclear rDNA evidence for major lineages of helenioid Heliantheae (Compositae). *Systematic Botany* 27: 161–198.

Bankevich A, Nurk S, Antipov D, Gurevich AA, Dvorkin M, Kulikov AS, Lesin VM, Nikolenko SI, Pham S, Prjibelski AD, Pyshkin AV. 2012. SPAdes: A new genome assembly algorithm and its applications to single-cell sequencing. *Journal of Computational Biology* 19: 455–477.

Barker MS, Kane NC, Matvienko M, Kozik A, Michelmore RW, Knapp SJ, Rieseberg LH. 2008. Multiple paleopolyploidizations during the evolution of the Compositae reveal parallel patterns of duplicate gene retention after millions of years. *Molecular Biology and Evolution* 25: 2445–2455.

Barker MS, Li Z, Kidder TI, Reardon CR, Lai Z, Oliveira LO, Scascitelli M, Rieseberg LH. 2016. Most Compositae (Asteraceae) are descendants of a paleohexaploid and all share a paleotetraploid ancestor with the Calyceraceae. *American Journal of Botany* 103: 1203–1211.

Barrier M, Baldwin BG, Robichaux RH, Purugganan MD. 1999. Interspecific hybrid ancestry of a plant adaptive radiation: allopolyploidy of the Hawaiian silversword alliance (Asteraceae) inferred from floral homeotic gene duplications. *Molecular Biology and Evolution* 16: 1105–1113.

Bentham G. 1844. *The botany of the voyage of the H.M.S. Sulphur, under the command of Captain Sir Edward Belcher, RN, CB, FRGS, etc., during the years 1836–42.* London: Smith Elder & Company.

Bertelsen CD. 2018. Thirty-seven years on a mountain trail: Vascular flora and flowering phenology of the Finger Rock Canyon Watershed, Santa Catalina Mountains, Arizona. *Desert Plants* 34: 6–248.

Bolger AM, Lohse M, Usadel B. 2014. Trimmomatic: A flexible trimmer for Illumina sequence data. *Bioinformatics* 30: 2114–2120.

Bonifacino JM, Robinson HE, Funk VA, Lack HW, Wagenitz G, Feuillet C, Hind DN. 2009. A history of research in Compositae: Early beginnings to the Reading Meeting (1975). In: Funk VA, Susanna A, Stuessy TF, Bayer RJ eds. *Systematics, evolution, and biogeography of Compositae.* Vienna: International Association for Plant Taxonomy, Institute of Botany, University of Vienna.

Burns KC. 2018. Time to abandon the loss of dispersal ability hypothesis in island plants: Comment on García-Verdugo, Mairal, Monroy, Sajeva and Caujapé-Castells (2017). *Journal of Biogeography* 45: 1219–1222.

Brandrud MK, Baar J, Lorenzo MT, Athanasiadis A, Bateman RM, Chase MW, Hedrén M, Paun O. 2020. Phylogenomic relationships of diploids and the origins of allotetraploids in *Dactylorhiza* (Orchidaceae). *Systematic Biology* 69: 91–109.

Cacho NI, Strauss SY. 2014. Occupation of bare habitats, an evolutionary precursor to soil specialization in plants.
Proceedings of the National Academy of Sciences of the United States of America 111: 15132–15137.

Capella-Gutiérrez S, Silla-Martínez JM, Gabaldón T. 2009. trimAl: A tool for automated alignment trimming in large-scale phylogenetic analyses. *Bioinformatics* 25: 1972–1973.

Carlquist S. 1974. *Island biology.* New York: Columbia University Press.

Carrillo-Reyes P. 2008. A new species of *Perityle* (Asteraceae, Perityleae) from western Mexico. *Systematic Botany* 33: 459–461.

Cassini H. 1829. Tableau synoptique des Synanthérées. *Annales des Sciences Naturelles (Paris)* 17: 387–423.

Cody ML, Overton JM. 1996. Short-term evolution of reduced dispersal in island plant populations. *Journal of Ecology* 84: 53–61.

Dodsworth S. 2015. Genome skimming for next-generation biodiversity analysis. *Trends in Plant Science* 20: 525–527.

Doyle JJ, Doyle JL. 1987. CTAB DNA extraction in plants. *Phytochemical Bulletin* 19: 11–15.

Everly ML. 1947. *A taxonomic study of the genus* Perityle *and related genera.* Stanford, CA, USA: Natural History Museum of Stanford University 3(12).

Faircloth BC. 2016. PHYLUCE is a software package for the analysis of conserved genomic loci. *Bioinformatics* 32: 786–788.

Fine PV, Mesones I, Coley PD. 2004. Herbivores promote habitat specialization by trees in Amazonian forests. *Science* 305: 663–665.

Fine PV, Miller ZJ, Mesones I, Irazuzta S, Appel HM, Stevens MH, Sääksjärvi I, Schultz JC, Coley PD. 2006. The growth–defense trade-off and habitat specialization by plants in Amazonian forests. *Ecology* 87: 150–162.

Freyman WA, Höhna S. 2018. Cladogenetic and anagenetic models of chromosome number evolution: A Bayesian model averaging approach. *Systematic Biology* 67: 195–215.

Freyman WA, Johnson M, Rothfels CJ. 2020. homologizer: A tree-based method for phasing evolutionary histories across loci. *bioRxiv.* https://doi.org/10.1101/2020.10.22.351486

Funk VA, Susanna A, Steussy TF, Robinson HE. 2009a. Classification of Compositae. In: Funk VA, Susanna A, Stuessy TF, Bayer RJ eds. *Systematics, evolution, and biogeography of Compositae.* Vienna: International Association for Plant Taxonomy, Institute of Botany, University of Vienna. 746–777.

Funk VA, Anderberg AA, Baldwin BG, Bayer RJ, Bonifacino JM, Breitwieser I, Brouillet L, Carbajal R, Chan R, Coutinho AX, Crawford DJ. 2009b. Compositae metatrees: The next generation. In: Funk VA, Susanna A, Stuessy TF, Bayer RJ eds. *Systematics, evolution, and biogeography of Compositae.* Vienna: International Association for Plant Taxonomy, Institute of Botany, University of Vienna.

Funk VA, Edwards R, Keeley S. 2018. The problem with (out) vouchers. *Taxon* 67: 3–5.

Gardner EM, Johnson MG, Pereira JT, Puad AS, Arifiani D, Sahromi S, Wickett NJ, Zerega NJ. 2019. Paralogs and off-target sequences improve phylogenetic resolution in a densely-sampled study of the breadfruit genus (*Artocarpus*, Moraceae). *bioRxiv.* https://doi.org/10.1101/854232

Glenn TC, Nilsen RA, Kieran TJ, Sanders JG, Bayona-Vásquez NJ, Finger JW, Pierson TW, Bentley KE, Hoffberg SL, Louha S, Garcia-De, Leon FJ. 2019. Adapterama I: Universal stubs and primers for 384 unique dual-indexed or 147,456 combinatorially-indexed Illumina libraries (iTru & iNext). *PeerJ (Corta Madera, CA and London)* 7: e7755.

Glick L, Mayrose I. 2014. ChromEvol: assessing the pattern of chromosome number evolution and the inference of polyploidy along a phylogeny. *Molecular Biology and Evolution* 31: 1914–1922.

Gray A. 1852. Plantae Wrightianae Texano—Neo-Mexicanae. *Smithsonian Contributions to Botany* 3: 99–101.

Heled J, Drummond AJ. 2009. Bayesian inference of species trees from multilocus data. *Molecular Biology and Evolution* 27: 570–580.

Herrando-Moraira S, Calleja JA, Galbany-Casals M, Garcia-Jacas N, Liu JQ, López-Alvarado J, López-Pujol J, Mandel JR, Massó S, Montes-Moreno N, Roquet C. 2019. Nuclear and plastid DNA phylogeny of tribe Cardueae (Compositae) with Hyb-Seq data: A new subtribal classification and a temporal diversification framework. *Molecular Phylogenetics and Evolution* 137: 313–332.

Heywood VH. 2009. The recent history of Compositae systematics: from daisies to deep achenes, sister groups and metatrees. In: Funk VA, Susanna A, Stuessy TF, Bayer RJ eds. *Systematics, evolution and biogeography of Compositae.* Vienna: International Association for Plant Taxonomy, Institute of Botany, University of Vienna. 39–44.

Höhna S, Landis MJ, Heath TA, Boussau B, Lartillot N, Moore BR, Huelsenbeck JP, Ronquist F. 2016. RevBayes: Bayesian phylogenetic inference using graphical models and an interactive model-specification language. *Systematic Biology* 65: 726–736.

Hopper SD. 2009. OCBIL theory: Towards an integrated understanding of the evolution, ecology and conservation of biodiversity on old, climatically buffered, infertile landscapes. *Plant and Soil* 322: 49–86.

Huang CH, Zhang C, Liu M, Hu Y, Gao T, Qi J, Ma H. 2016. Multiple polyploidization events across Asteraceae with two nested events in the early history revealed by nuclear phylogenomics. *Molecular Biology and Evolution* 33: 2820–2835.

Huelsenbeck JP, Rannala B, Masly JP. 2000. Accommodating phylogenetic uncertainty in evolutionary studies. *Science* 288: 2349–2350.

Huelsenbeck JP, Nielsen R, Bollback JP. 2003. Stochastic mapping of morphological characters. *Systematic Biology* 52: 131–158.

Huelsenbeck JP, Larget B, Alfaro ME. 2004. Bayesian phylogenetic model selection using reversible jump Markov chain Monte Carlo. *Molecular Biology and Evolution* 21: 1123–1133.

Jeffrey C. 2007. Evolution of Compositae flowers. In: Funk VA, Susanna A, Stuessy TF, Bayer RJ eds. *Systematics, evolution and biogeography of Compositae.* Vienna: International Association for Plant Taxonomy, Institute of Botany, University of Vienna. 131–138.

Jones KE, Fér T, Schmickl RE, Dikow RB, Funk VA, Herrando-Moraira S, Johnston PR, Kilian N, Siniscalchi CM, Susanna A, Slovák M. 2019. An empirical assessment of a single family-wide hybrid capture locus set at multiple evolutionary timescales in Asteraceae. *Applications in Plant Sciences* 7: e11295.

Katoh K, Asimenos G, Toh H. 2009. Multiple alignment of DNA sequences with MAFFT. In: Posada D ed. *Bioinformatics for DNA sequence analysis.* Totowa, NJ: Humana Press. 39–64.

Larson DW, Matthes U, Kelly PE. 2005. *Cliff ecology: Pattern and process in cliff ecosystems.* Cambridge: Cambridge University Press.

Li H, Durbin R. 2010. Fast and accurate long-read alignment with Burrows–Wheeler transform. *Bioinformatics* 26: 589–595.

Maddison WP. 1997. Gene trees in species trees. *Systematic Biology* 46: 523–536.

Mandel JR, Barker MS, Bayer RJ, Dikow RB, Gao TG, Jones KE, Keeley S, Kilian N, Ma H, Siniscalchi CM, Susanna A. 2017. The Compositae tree of life in the age of phylogenomics. *Journal of Systematics and Evolution* 55: 405–410.

Mandel JR, Dikow RB, Funk VA. 2015. Using phylogenomics to resolve mega-families: an example from Compositae. *Journal of Systematics and Evolution* 53: 391–402.

Mandel JR, Dikow RB, Funk VA, Masalia RR, Staton SE, Kozik A, Michelmore RW, Rieseberg LH, Burke JM. 2014. A target enrichment method for gathering phylogenetic information from hundreds of loci: An example from the Compositae. *Applications in Plant Sciences* 2: 1300085.

Mandel JR, Dikow RB, Siniscalchi CM, Thapa R, Watson LE, Funk VA. 2019. A fully resolved backbone phylogeny reveals numerous dispersals and explosive diversifications throughout the history of Asteraceae. *Proceedings of the National Academy of Sciences of the United States of America* 116: 14083–14088.

Mayrose I, Barker MS, Otto SP. 2010. Probabilistic models of chromosome number evolution and the inference of polyploidy. *Systematic Biology* 59: 132–144.

Meier JI, Marques DA, Mwaiko S, Wagner CE, Excoffier L, Seehausen O. 2017. Ancient hybridization fuels rapid cichlid fish adaptive radiations. *Nature Communications* 8: 14363.

Miller MA, Pfeiffer W, Schwartz T. 2010. Creating the CIPRES Science Gateway for inference of large phylogenetic trees. In: *Proceedings of the Gateway Computing Environments Workshop (GCE).* New Orleans, LA. 1–8.

Niles WE. 1970. *Taxonomic investigations in the genera* Perityle *and* Laphamia *(Compositae).* Memoirs of the New York Botanical Garden. No. 580.

Panero JL. 2007. Heliantheae Alliance: Tribe Perityleae Baldwin. In: Kadereit JW, Jeffrey C eds. *Flowering plants. Eudicots. The families and genera of vascular plants.* Berlin, Heidelberg: Springer. 8: 417–420.

Panero JL, Crozier BS. 2016. Macroevolutionary dynamics in the early diversification of Asteraceae. *Molecular Phylogenetics and Evolution* 99: 116–132.

Panero JL, Freire SE, Espinar LA, Crozier BS, Barboza GE, Cantero JJ. 2014. Resolution of deep nodes yields an improved backbone phylogeny and a new basal lineage to study early evolution of Asteraceae. *Molecular Phylogenetics and Evolution* 80: 43–53.

Panero J, Funk VA. 2002. Toward a phylogenetic subfamilial classification for the Compositae (Asteraceae). *Proceedings of the Biological Society of Washington* 115: 760–773.

Panero JL, Funk VA. 2008. The value of sampling anomalous taxa in phylogenetic studies: Major clades of the Asteraceae revealed. *Molecular Phylogenetics and Evolution* 47: 757–782.

Pouchon C, Fernández A, Nassar JM, Boyer F, Aubert S, Lavergne S, Mavárez J. 2018. Phylogenomic analysis of the explosive adaptive radiation of the *Espeletia* complex (Asteraceae) in the tropical Andes. *Systematic Biology* 67: 1041–1460.

Powell AM. 1968a. Additional discussions pertaining to the congeneric status of *Perityle* and *Laphamia* (Compositae). *SIDA, Contributions to Botany* 3: 270–278.

Powell AM. 1968b. Chromosome numbers in *Perityle* and related genera (Peritylanae–Compositae). *American Journal of Botany* 55: 820–828.

Powell AM. 1969. Taxonomy of *Perityle* section *Pappothrix* (Compositae–Peritylanae). *Rhodora* 71: 58–93.

Powell AM. 1970. Natural intersectional hybridization in *Perityle* (Compositae). *Brittonia* 22: 3–10.

Powell AM. 1972a. Taxonomy of *Amauria* (Compositae–Peritylinae). *Madroño* 21: 516–525.

Powell AM. 1972b. New species of *Perityle* and *Amauria* (Compositae). *Madroño* 21: 456–458.

Powell AM. 1972c. Artificial hybridizations in the subtribe Peritylanae (Compositae–Helenieae). *American Journal of Botany* 59: 760–768.

Powell AM. 1973a. Taxonomy of *Perityle* section *Laphamia* (Compositae–Helenieae–Peritylinae). *SIDA, Contributions to Botany* 5: 61–128.

Powell AM. 1973b. Taxonomy of *Pericome* (Compositae–Peritylinae). *The Southwestern Naturalist* 18: 335–339.

Powell AM. 1974. Taxonomy of *Perityle* section *Perityle* (Compositae–Peritylinae). *Rhodora* 76: 229–306.

Powell AM. 1976. New species of *Perityle* (Asteraceae) from Coahuila, Mexico. *Sida, Contributions to Botany* 6: 311–312.

Powell AM. 1983. *Perityle* (Asteraceae), new species and notes. *Madroño* 30: 217–225.

Powell AM, Kyhos DW, Raven PH. 1975. Chromosome numbers in Compositae. XI. Helenieae. *American Journal of Botany* 62: 1100–1103.

Powell AM, Sikes S. 1970. Chromosome numbers of some Chihuahuan desert Compositae. *The Southwestern Naturalist* 15: 175–186.

Powell AM, Turner BL. 1974. A generic conspectus of the subtribe Peritylinae (Asteraceae–Helenieae) and reassessment of its tribal position. *American Journal of Botany* 61: 87–93.

Rajakaruna N. 2018. Lessons on evolution from the study of edaphic specialization. *The Botanical Review* 84: 39–78.

Rambaut A, Drummond AJ, Xie D, Baele G, Suchard MA. 2018. Posterior summarization in Bayesian phylogenetics using Tracer 1.7. *Systematic Biology* 67: 901–904.

Revell LJ. 2012. phytools: An R package for phylogenetic comparative biology (and other things). *Methods in Ecology and Evolution* 3: 217–223.

Rieseberg LH, Soltis DE. 1991. Phylogenetic consequences of cytoplasmic gene flow in plants. *Evolutionary Trends in Plants* 5: 65–84.

Rice A, Glick L, Abadi S, Einhorn M, Kopelman NM, Salman-Minkov A, Mayzel J, Chay O, Mayrose I. 2015. The Chromosome Counts Database (CCDB)–A community resource of plant chromosome numbers. *New Phytologist* 206: 19–26.

Robinson HE. 1981. A revision of the tribal and subtribal limits of the Heliantheae (Asteraceae). *Smithsonian Contributions to Botany* 51: 1–102.

Robinson HE, Powell AM, King RM, Weedin JF. 1981. Chromosome numbers in the Compositae. *XII: Heliantheae. Smithsonian Contributions to Botany* 52: 1–28.

Robinson HE, Schilling E, Panero JL. 2007. Eupatorieae. In: Funk VA, Susanna A, Stuessy TF, Bayer RJ eds. *Systematics, evolution and biogeography of Compositae.* Vienna: International Association for Plant Taxonomy, Institute of Botany, University of Vienna. 731–744.

Rydberg PA. 1914. Carduaceae–Helenieae–Peritylanae. *North American Flora* 34: 11–27.

Sayyari E, Whitfield JB, Mirarab S. 2018. DiscoVista: Interpretable visualizations of gene tree discordance. *Molecular Phylogenetics and Evolution* 122: 110–115.

Schliep KP. 2011. phangorn: Phylogenetic analysis in R. *Bioinformatics* 27: 592–593.

Shinners LH. 1959. Species of *Laphamia* transferred to *Perityle* (Compositae–Helenieae). *The Southwestern Naturalist* 4: 204–206.

Siniscalchi CM, Loeuille B, Funk VA, Mandel JR, Pirani JR. 2019. Phylogenomics yields new insight into relationships within Vernonieae (Asteraceae). *Frontiers in Plant Science* 10: 1224.

Smith BT, Harvey MG, Faircloth BC, Glenn TC, Brumfield RT. 2014. Target capture and massively parallel sequencing of ultra-conserved elements for comparative studies at shallow evolutionary time scales. *Systematic Biology* 63: 83–95.

Spellenberg R, Powell AM. 1990. A new species of *Perityle* (Asteraceae) from southwestern Chihuahua, Mexico. *Systematic Botany* 15: 252–255.

Stamatakis A. 2014. RAxML version 8: A tool for phylogenetic analysis and post-analysis of large phylogenies. *Bioinformatics* 30: 1312–1313.

Stuessy TF, Garver D. 1994. The defensive role of pappus in heads of Compositae. In: Caligari PDS, Hind DJN eds. *Compositae: Biology and utilization. Proceedings of the International Compositae Conference, Kew,* 1994, Kew: Royal Botanic Gardens. 2: 81–91.

Straub SC, Parks M, Weitemier K, Fishbein M, Cronn RC, Liston A. 2012. Navigating the tip of the genomic iceberg: Next-generation sequencing for plant systematics. *American Journal of Botany* 99: 349–364.

Strauss SY, Cacho NI. 2013. Nowhere to run, nowhere to hide: the importance of enemies and apparency in adaptation to harsh soil environments. *The American Naturalist* 182: 1–4.

Susanna A, Jacas NG, Soltis DE, Soltis PS. 1995. Phylogenetic relationships in tribe Cardueae (Asteraceae) based on ITS sequences. *American Journal of Botany* 82: 1056–1068.

Thapa R, Bayer RJ, Mandel JR. 2020. Phylogenomics resolves the relationships within *Antennaria* (Asteraceae, Gnaphalieae) and yields new insights into its morphological character evolution and biogeography. *Systematic Botany* 45: 387–402.

Todsen TK. 1974. A new species of *Perityle* (Compositae) from Arizona. *Journal of the Arizona Academy of Science* 9: 35.

Todsen TK. 1983. A new variety of *Perityle staurophylla* (Asteraceae) from New Mexico. *Madroño* 30: 115–117.

Turner BL. 1966. Taxonomy of *Eutetras* (Compositae: Helenieae). *The Southwestern Naturalist* 11: 118–122.

Turner BL. 1989. New species and combinations in *Perityle* (Asteraceae) from northwestern Mexico. *Phytologia* 66: 504–506.

Turner BL. 2013. Chapter 13: Tribes Madieae and Perityleae. Robert, Adams, In: *The Comps of Mexico. A systematic account of the family Asteraceae. Phytologia memoirs.* Austin: Plant Resource Center, The University of Texas at Austin. 23–70.

Vargas OM, Ortiz EM, Simpson BB. 2017. Conflicting phylogenomic signals reveal a pattern of reticulate evolution in a recent high-Andean diversification (Asteraceae: Astereae: *Diplostephium*). *New Phytologist* 214: 1736–1750.

Watson LE, Siniscalchi CM, Mandel J. 2020. Phylogenomics of the hyperdiverse daisy tribes: Anthemideae, Astereae, Calenduleae, Gnaphalieae, and Senecioneae. *Journal of Systematics and Evolution* 58: 841–852.

Weitemier K, Straub SC, Cronn RC, Fishbein M, Schmickl R, McDonnell A, Liston A. 2014. Hyb-Seq: Combining target enrichment and genome skimming for plant phylogenomics. *Applications in Plant Sciences* 2: 1400042.

Welsh SL, Neese E. 1983. New species of *Hymenoxys* and *Perityle* (Compositae) from Utah. *Great Basin Naturalist* 43: 6.

Yarborough SC, Powell AM. 2006. Perityle. In: Flora of North America Editorial Committee ed. *Flora of North America North of Mexico*. New York and Oxford: Oxford University Press. 21: 316–335.

Zhang C, Rabiee M, Sayyari E, Mirarab S. 2018. ASTRAL-III: Polynomial time species tree reconstruction from partially resolved gene trees. *BMC Bioinformatics* 19: 153.

Supplementary Material

The following supplementary material is available online for this article at http://onlinelibrary.wiley.com/doi/10.1111/jse.12711/suppinfo:

Fig. S1. Maximum likelihood phylogeny of Perityleae based on whole chloroplast genomes inferred using RAxML (Stamatakis, 2014) on XSEDE through the CIPRES Science Gateway portal (Miller et al., 2010) using the GTRCAT model of molecular substitution and 1000 bootstrap replicates.

Fig. S2. Maximum a posteriori phylogenetic tree of Perityleae based on whole chloroplast genomes compiled from 30 000 generations of an MCMC in RevBayes (Höhna et al., 2016) conditioned on a GTR + gamma + I model of molecular substitution with four discrete rate categories.

Fig. S3. Maximum likelihood phylogeny of Perityleae based on the nuclear ribosomal cistron inferred using RAxML (Stamatakis, 2014) on XSEDE through the CIPRES Science Gateway portal (Miller et al., 2010) using the GTRCAT model of molecular substitution and 1000 bootstrap replicates.

Fig. S4. Maximum a posteriori phylogeny of Perityleae based on nuclear ribosomal cistrons compiled from a posterior distribution of trees generated during 30 000 iterations of an MCMC in RevBayes (Höhna et al., 2016) conditioned on a GTR + Gamma + I model of molecular substitution with four discrete rate categories.

Fig. S5. Maximum likelihood phylogeny of Perityleae based on a concatenated matrix of 212 orthologous low-copy nuclear loci inferred using RAxML (Stamatakis, 2014) on XSEDE through the CIPRES Science Gateway portal (Miller et al., 2010) using the GTRCAT model of molecular substitution and 1000 bootstrap replicates.

Fig. S6. Maximum a posteriori phylogeny of Perityleae based on a concatenated matrix of 212 orthologous low-copy nuclear loci compiled from a posterior distribution of trees generated during 30 000 generations of an MCMC in RevBayes (Höhna et al., 2016) conditioned on a GTR + Gamma + I model of molecular substitution with four discrete rate categories.

Fig. S7. Multi-species pseudocoalescent tree of Perityleae inferred using ASTRAL-III (Zhang et al., 2018) to account for gene-tree discordance from 212 gene trees inferred separately in RAxML (Stamatakis, 2014) using the GTRCAT model of molecular substitution and 1000 bootstrap replicates.

Fig. S8. Maximum likelihood reconstruction of ancestral chromosome numbers (**A**) and model-averaged maximum a posteriori ancestral state reconstructions (**B**–**I**) of morphological traits traditionally emphasized in Perityleae classification based on the posterior of trees from the Bayesian analysis of whole chloroplast genomes. **A,** Ancestral chromosome numbers were reconstructed under the CONST_RATE_DEMI_EST model in the software program ChromEvol (Mayrose et al., 2010; Glick & Mayrose, 2014) on the map phylogenetic tree based on whole chloroplast genomes. Tips that are missing color-coded labels are of unknown chromosome number. **B**–**I,** Maximum a posteriori ancestral states reconstructions were compiled from a posterior distribution of 1200 stochastic character maps generated using reversible jump MCMC in RevBayes (Höhna et al., 2016). Stochastic character maps were conditioned on two plausible models for each transition rate, either a reversible (non-zero) or an irreversible (zero) rate, and mapped on a posterior distribution of 604 trees generated by our Bayesian inference of tree topology based on whole chloroplast genomes.

Fig. S9. Model-averaged posterior densities of transition rates between morphological character states for traits traditionally emphasized in classification of Perityleae. Transition rates are reported in changes per unit branch length.

Fig. S10. Maximum likelihood based reconstruction of ancestral chromosome numbers in Perityleae with *Galeana pratensis* ($x = 9$) removed from the analysis to examine sensitivity of the root chromosome number to the earliest diverging lineage. Ancestral chromosome numbers were inferred under the CONST_RATE_DEMI_EST model in the software program ChromEvol (Mayrose et al., 2010; Glick & Mayrose, 2014) onto the MAP phylogenetic tree from our Bayesian analysis of combined nrDNA and low-copy nuclear loci. Node labels denote node order and maximum likelihood ancestral chromosome numbers.

Data S1. Phylogenomics of Perityleae (Compositae) provides new insights into morphological and chromosomal evolution of the rock daisies, Dryad, Dataset, available from the Dryad Digital Repository: https://doi.org/10.5061/dryad.fn2z34tsg

Appendix I

Voucher information, and GenBank SRA accession numbers for sampled individuals of Perityleae and outgroups. Herbarium acronyms follow Thiers, B. [continuously updated]. Index Herbariorum: A global directory of public herbaria and associated staff. New York Botanical Garden's Virtual Herbarium. http://sweetgum.nybg.org/science/ih/

Taxon	Accession or collection #	Location	Herbarium	Collector(s)	Collection date	GenBank SRA #
Galeana pratensis (Kunth.) Rydb.	US2756473	Mexico: Jalisco, 1.3 mi NNE of Santa Cruz on rte 15	UC	Stuessy, T. F.; Gardner, R. C.	9/2/73	PRJNA673739 SAMN16622012
Eutetras pringlei A. Gray	CAS915298	Mexico: Queretaro, Cadereyta de Montes	UC	S. Zamudio	10/25/1988	PRJNA673739 SAMN16622013
Eutetras palmeri Greenm.	UCR117599	Mexico: Aguascalientes	UCR	Jose Luis Villaseñor & J.I. Calzada	10/22/95	PRJNA673739 SAMN16622014
Pericome caudata A. Gray	UC2027235	USA: California, Inyo co. White mountains, Silver canyon,	UC	D. Keil	9/20/1988	PRJNA673739 SAMN16622015
Pericome caudata A. Gray	ILM769	USA: Arizona, Chiricahua mountains	UC	I.H. Lichter-Marck, J. Santore	9/14/2019	PRJNA673739 SAMN16622016
Pericome caudata A. Gray	ILM316	USA: Arizona, San Francisco peaks	UC	I.H. Lichter-Marck	9/29/2018	PRJNA673739 SAMN16622017
Amauria rotundifolia Benth.		USA: California	US	Edwards, R.D	9/6/16	PRJNA540287 SAMN11585449
Amauria rotundifolia Benth.	UC1298184	Mexico: Baja California Sur, On cliffs at north side of the steep east arroyo, Volcan las Tres Virgenes.	UC	R. Moran	2/12/64	PRJNA540287 SAMN11585449
Amauria carterae A.M. Powell	SD160154	Mexico: Baja California Sur. Sierra la Giganta	SD	Miguel Domínguez León	10/12/2004	PRJNA673739 SAMN16622018
Amauria brandegeeana (Rose) Rydb.	UCR146783	Mexico: Baja California Sur. Vizcaino Desert, north of El Arco and north of Calmalli, along road between Rancho Esperanza and Rancho Miramar	UCR	Jon P. Rebman, N. Roberts	3/11/98	PRJNA673739 SAMN16622019
Perityle californica Benth.	UC1787616	Mexico: Baja California Sur, 1.5 mile E of Ley Federal de Aguas Numero Cinco, along road to Rancho Tijuana; E of Ciudad Constitucion.	UC	Jon P. Rebman	10/24/01	PRJNA673739 SAMN16622020
Perityle californica Benth.	ILM 692	Mexico: Baja California Sur, San Ignacio	UC	I.H. Lichter-Marck	12/7/2018	PRJNA673739 SAMN16622021
Perityle cuneata Brandegee	UC116153	Mexico: Baja Califoria Sur, Coyote beach	UC	D. Porter	12/30/1958	PRJNA673739 SAMN16622022
Perityle cuneata Brandegee	ILM 677	Mexico: Baja California Sur, Sierra de la Laguna	UC	I.H. Lichter Marck	12/6/2018	PRJNA673739 SAMN16622023
Perityle crassifolia Brandegee var. *crassifolia*	UTH 59936	Mexico: Baja California Sur, Isla Coronado	UTH	Ira L. Wiggins	4/3/1976	PRJNA673739 SAMN16622024
Perityle crassifolia Brandegee var. *crassifolia*	ILM 674	Mexico: Baja California Sur, Las Ventanas	UC	I.H. Lichter-Marck	12/4/2018	PRJNA673739 SAMN16622025
Perityle crassifolia var. *robusta* (Rydb.) Everly	ILM 661	Mexico: Baja California Sur, La Paz-Tecolote rd	UC	I.H. Lichter-Marck	12/1/2018	PRJNA673739 SAMN16622026
Perityle coronopifolia A. Gray	ILM 276	USA: Arizona, Patagonia mountains	UC	I.H. Lichter-Marck, A. Baniaga	9/14/2018	PRJNA673739 SAMN16622027
Perityle coronopifolia	UC 1608506	USA: New Mexico, Luna Co., Summit of Cookes peak	UC	J. Travis Colombus	7/18/1986	PRJNA673739 SAMN16622028

Appendix I Continued

Taxon	Accession or collection #	Location	Herbarium	Collector(s)	Collection date	GenBank SRA #
A. Gray						
Perityle ciliata (L.H. Dewey) Rydb.	UC 1523877	USA: Coconino co., Flagstaff, Elden mtn.	UC	J. Morefield	7/29/1985	PRJNA673739 SAMN16622029
Perityle ciliata (L.H. Dewey) Rydb.	ILM 875	USA: Arizona, Prescott	UC	I.H. Lichter-Marck, S. Winitsky	9/10/2019	PRJNA673739 SAMN16622030
Perityle vigilans Spellenb. & A.M. Powell	UC 1555785	Mexico: Chihuahua, Maguarichi, At Maguarichi and to 3 mi NE along road	UC	R.W. Spellenberg, R. Soreng, R. Corral-Díaz, and T.K. Todsen	4/28/85	PRJNA673739 SAMN16622031
Perityle microglossa Benth. var. *microglossa*	CAS 622498	Mexico: Durango	CAS	D.E. Breedlove	9/17/1979	PRJNA673739 SAMN16622032
Perityle turneri A.M. Powell	UC 1523224	Mexico: Chihuahua,	UC	G. Nesom, P. Lewis	8/25/1984	PRJNA673739 SAMN16622033
Perityle turneri A.M. Powell	ILM 656	Mexico: Durango, Mexiquilla del alto	UC	I.H.Lichter-Marck, A. Castro-Castro	11/22/2018	PRJNA673739 SAMN16622034
Perityle feddemae McVaugh	NY 426075	Mexico: Zacatecas, 7.2 mi W of Valparaiso, Zac.	NYBG	B. L. Turner	8/16/69	PRJNA673739 SAMN16622035
Perityle feddemae McVaugh	ILM 656	Mexico: Jalisco, Mpio.	UC	I.H. Lichter-Marck, P. Carillo-Reyes	11/10/2018	PRJNA673739 SAMN16622036
Perityle microcephala A. Gray	UC 1717054	Mexico: Chihuahua, MPIO. Chihuahua on the road to Cumbre de Majalaca	UC	R. Spellenberg, N. Zucker	11/25/1990	PRJNA673739 SAMN16622037
Perityle hofmeisteria Rydb.	Lundell 60070	Mexico: Durango, Mapimi. Sierra el Rosario	Lundell	T.L. Wendt, F. Chiang, & M.C. Johnston	11/2/1972	PRJNA673739 SAMN16622038
Perityle hofmeisteria Rydb.	ILM 640	Mexico: Durango, Nombre de Dios	UC	I.H. Lichter-Marck, A. Castro Castro	11/21/2018	PRJNA673739 SAMN16622039
Perityle trichodonta S.F. Blake	UCR 70576	Mexico: Nayarit, a 22.7 km al SW de Jesus Maria, camino a la Mesa del Nayar.	UCR	O. Téllez V., G. Flores F.	11/5/88	PRJNA673739 SAMN16622040
Perityle trichodonta S.F. Blake	ILM 615	Mexico: Jalisco, Bolaños,	UC	I.H. Lichter-Marck, P. Carillo-Reyes	11/1/2018	PRJNA673739 SAMN16622041
Perityle gentryi A.M. Powell	ASU0028881	Mexico: Sonora, Alamos	ASU	T. R. Van Devender, A. L. Reina G., B. E. Loyola G., M. A. Dimmitt	10/1/06	PRJNA673739 SAMN16622042
Perityle batopilensis A.M. Powell	SRSC 14484	Mexico: Chihuahua, Batopilas, On Batopilas-Urique-Samachique Rd. NW of Batopilas 8.6 road km above crossing of Rio Batopilas	SRSC	R. Spellenberg, W. Anderson	9/25/2012	PRJNA673739 SAMN16622043
Perityle montana (A.M. Powell) B.G. Baldwin	UC 1523222	Mexico: Chihuahua, Sierra Mohinora	UC	D.S. Correll, H.S. Gentry	10/16/1959	PRJNA673739 SAMN16622044
Perityle rosei Greenm.	CAS 694453	Mexico: Durango, 45 km west of Heujuquilla del alto	CAS	D.E. Breedlove, F. Almeda	11/23/1983	PRJNA673739 SAMN16622045
Perityle harkerae	UTH 450757	Mexico: Zacatecas, Teul de	UTH	P.Carrillo-Reyes,	4/22/2010	PRJNA673739

www.jse.ac.cn

J. Syst. Evol. 58(6): 853–880, 2020

Appendix I Continued

Taxon	Accession or collection #	Location	Herbarium	Collector(s)	Collection date	GenBank SRA #
P. Carillo		Gonazalez Ortega		A. Castro-Castro		SAMN16622046
Perityle glaucescens B.L. Turner	UTH 29908	Mexico: Zacatecas, Juchicila	UTH	J.L. Panero, I. Calzada, J.F. Ortega, A. Santos	11/7/19996	PRJNA673739 SAMN16622047
Perityle canescens Everly	UC 651747	Mexico: Sinaloa, Capadero, Sierra Tacuichamona	UC	H.S. Gentry	2/12/1940	PRJNA673739 SAMN16622048
Perityle lineariloba Rydb.	UC 145620	Mexico: Durango, San Ramon	UC	E. Palmer	4/21/1906	PRJNA673739 SAMN16622049
Perityle ajoensis T.K. Todsen	AZ 415913	United States, Arizona, Pima County, Ajo mtns.	AZ	Sue Rutman	9/22/13	PRJNA673739 SAMN16622050
Perityle incana A. Gray	UCR 59009	Mexico: Baja California Norte, Ensenada, Guadalupe Island, Islote Negro	UCR	Reid Moran	4/18/70	PRJNA673739 SAMN16622051
Perityle incana A. Gray	ILM 1011	USA: California, UCLA Botanical Garden cultivar	UC	I.H. Lichter-Marck, E. Meyer	6/3/2019	PRJNA673739 SAMN16622052
Perityle lobata (Rydb.) I.M. Johnston	AZ 389706	Mexico: Baja California Sur, Sierra de La Giganta. Rancho La Banderita, Mesa de Humi.	AZ	Jose Luis Leon de la Luz	3/3/2005	PRJNA673739 SAMN16622053
Perityle lobata (Rydb.) I.M. Johnston	ILM 682	Mexico: Baja California Sur, Sierra la Giganta, Mesa Tinajas	UC	I.H. Lichter-Marck, Juan Polo Luis Higuera	12/6/018	PRJNA673739 SAMN16622054
Perityle emoryi Torr.	UC 648836	Chile: Antofogasta	UC	A.A. Beetle	2/9/1939	PRJNA673739 SAMN16622055
Perityle emoryi Torr.	ILM2017-2	Mexico: Baja California Norte, Ejido Erendira	UC	I.H. Lichter-Marck	5/13/2017	PRJNA673739 SAMN16622056
Perityle emoryi Torr.	JEPS 122488	USA: California, San Bernardino	JEPS	B.G. Baldwin, J. Strother		PRJNA673739 SAMN16622057
Perityle emoryi Torr.	ILM2017-3	Mexico: Baja California Norte, Bahia de Los Angeles	UC	I.H.Lichter-Marck	5/16/2017	PRJNA673739 SAMN16622058
Perityle emoryi Torr.	ILM 2018-3	California: Imperial coo, Chocolate Mountains	UC	I.H. Lichter-Marck, A. Sanders, J. Malusa	3/8/2017	PRJNA673739 SAMN16622059
Perityle palmeri S. Watson	ILM 547	Mexico: Sonora, Rancho Nuevo.	UC	I.H. Lichter-Marck, J. Pablo-Carillo	10/16/2018	PRJNA673739 SAMN16622060
Perityle palmeri S. Watson	UC1424077	Mexico: Sonora	UC	Unknown	1967	PRJNA673739 SAMN16622061
Perityle reinana B.L. Turner	AZ 384911	Mexico: Sonora, Municipio de Ures. Ca. 0.5 km below Aguaje in Canada El Carrizo, Sierra de Mazatán	AZ	A. L. Reina-G.	4/29/04	PRJNA673739 SAMN16622062
Perityle reinana B.L. Turner	ILM 265	Mexico: Sonora, Municipio de Ures. Ca. 0.5 km below Aguaje in Canada El Carrizo, Sierra de Mazatán	UC	I.H. Lichter-Marck, J. Sanchez-Escalante, R. Puente, R. Villa	8/11/2018	PRJNA673739 SAMN16622063
Perityle cordifolia (Rydb.) S.F. Blake	UC 1616144	Mexico: Sonora, Yécora, 2.7 km west-northwest of Tepoca on Mex. 16	UC	A.L. Reina-G., T.R. Van Devender, T.F. Daniel, G.M. Ferguson, B.J. Syke	3/17/98	PRJNA673739 SAMN16622064
Perityle leptoglossa	UC 1765926	Mexico: Sonora, road from Hermosillo to Ures	UC	L.R. Landrum, T. Nash, J. Poelt,	2/22/1987	PRJNA673739 SAMN16622065

Appendix I Continued

Taxon	Accession or collection #	Location	Herbarium	Collector(s)	Collection date	GenBank SRA #
Harv. & Gray ex. A. Gray				B. Ryan		
Perityle leptoglossa Harv. & Gray ex. A. Gray	ILM 544	Mexico: Sonora, Magdalena palm canyon	UC	I.H. Lichter-Marck, J. Pablo-Carillo	10/20/2018	PRJNA673739 SAMN16622066
Perityle vandevenderi B.L. Turner	AZ 276021	Mexico: Sonora, Magdalena palm canyon	AZ	M.R. Johnson	10/11/87	PRJNA673739 SAMN16622067
Perityle vandevenderi B.L. Turner	Vandevender 2018-87	Mexico: Sonora, Sierra el Baviso	US	M.R. Johnson	10/11/87	PRJNA673739 SAMN16622068
Perityle pseudociliata A.M. Powell & Yarborough	AZ 356412	Mexico: Chihuahua, Casas Grandes Municipality, 15 mi up Tinaja Wash from hwy junction; In Sierra La Brena on E slope of the Sierra Madre Occidental	AZ	J. Spencer, D. Atwood	9/25/98	PRJNA673739 SAMN16622069
Perityle cochisensis (W.E. Niles) A.M. Powell	AZ 364850	USA: Arizona, Cochise co., Chiricahua mtns.	AZ	M. Quinn, R. Ogden	9/27/2008	PRJNA673739 SAMN16622070
Perityle cochisensis (W.E. Niles) A.M. Powell	ILM 300	USA: Arizona, Cochise co., Chiricahua mtns. Cave Creek	UC	I.H. Lichter-Marck	8/23/2019	PRJNA673739 SAMN16622071
Perityle staurophylla (Barneby) Shinners	UC 1731838	USA: New Mexico, Otero co. Fresnal Cyn.	UC	D. Wm. Taylor	7/21/1991	PRJNA673739 SAMN16622072
Perityle megalocephala (S. Watson) J.F. Macbr. var. *megalocephala*	JEPS 89370	USA: California, Inyo, at the Narrows (Devils Gate, Waucoba rd. on w. slope Inyo Mts.); Inyo Mts., Devils Gate	UC	D. Wm. Taylor	10/22/1978	PRJNA673739 SAMN16622073
Perityle megalocephala (S. Watson) J.F. Macbr. var. *megalocephala*	ILM 122	USA: California, Inyo co. White mountains, Silver canyon,	UC	I.H. Lichter-Marck, S. Winitsky, J. Martinez-Gomez, S. Fram	7/3/2017	PRJNA673739 SAMN16622074
Perityle megalocephala (S. Watson) J.F. Macbr. var. *oligophylla* A.M. Powell	ILM 166	USA: California, Inyo co. Papoose flat	UC	I.H. Lichter-Marck, K. Allerton	6/12/2018	PRJNA673739 SAMN16622075
Perityle c.f. villosa (S.F. Blake) Shinners	UC 1971306	USA: California, Inyo co. Tin Mountain	UC	M. Dedecker	7/24/1978	PRJNA673739 SAMN16622076
Perityle villosa (S.F. Blake) Shinners	ILM 97	USA: California, Inyo co., Panamint mtns., Hanaupah canyon	UC	I.H. Lichter-Marck, K. Allerton	7/1/2018	PRJNA673739 SAMN16622077
Perityle inyoensis Ferris (A.M. Powell)	UC 697246	USA: California, Inyo co., Cerro Gordo pk.	UC	A.M. Alexander, L. Kellogg	7/4/1942	PRJNA673739 SAMN16622078
Perityle inyoensis Ferris (A.M.	ILM 2	USA: California, Inyo mtns., Santa Rosa mine	UC	I.H. Lichter-Marck, K.	6/26/2018	PRJNA673739 SAMN16622079

Appendix I Continued

Taxon	Accession or collection #	Location	Herbarium	Collector(s)	Collection date	GenBank SRA #
Powell)				Allerton		
Perityle gilensis (M.E. Jones) J.F. Macbr.	AZ 294925	USA: Arizona, Pinal County, Box Canyon, Mineral Mountain area, ca. 3 miles (by air) north of the Gila River, ca. 12. 5 miles east-northeast of Florence.	AZ	T. R. & R. K. Van Devender	2/22/92	PRJNA673739 SAMN16622080
Perityle gilensis (M.E. Jones) J.F. Macbr.	ILM-761	USA: Arizona, Gila co. Superstition mtns.	UC	I.H. Lichter-Marck, J. Santore	8/13/2019	PRJNA673739 SAMN16622081
Perityle coahuilensis A.M. Powell	AZ 337203	Mexico: Coahuila, 1.5 km northeast Ranco de San Marcos, on the western edge of the Sierra de San Marcos	AZ	M.C. Johnston, T.L. Wendt, F. Chiang	6/12/72	PRJNA673739 SAMN16622082
Perityle ambrosiifolia Green ex. A.M. Powell & Yarborough	AZ 378269	USA: Arizona, Greenlee County, Eagle Creek near Phelps Dodge pump station 6.6 road miles W. of Hwy 191 from Stargo turnoff; W. of Morenci, ca. 6 miles N of confluence with Gila River.	AZ	Lyle McGill	6/18/94	PRJNA673739 SAMN16622083
Perityle ambrosiifolia Green ex. A.M. Powell & Yarborough	ILM 467	USA: Arizona, Greenlee co., Eagle creek near Morenci	UC	I.H. Lichter-Marck	10/11/2018	PRJNA673739 SAMN16622084
Perityle lemmonii (A. Gray) J.F. MacBr.	UC 709590	USA: Arizona, Graham Mtns.	UC	B. Maguire, R.R. Maguire	6/2/1935	PRJNA673739 SAMN16622085
Perityle lemmonii (A. Gray) J.F. MacBr.	ILM 458	USA: New Mexico, Dona Ana co. Big Hatchet mountains	UC	I.H. Lichter-Marck	10/10/2018	PRJNA673739 SAMN16622086
Perityle gracilis (M.E. Jones) Rydb.	UC 1582885	USA: Nevada, Clark co. Sheep range. Joe May Canyon	UC	T.L. Ackerman	8/2/1979	PRJNA673739 SAMN16622087
Perityle gracilis (M.E. Jones) Rydb.	ILM 329	USA: Nevada, Condor canyon.	UC	I.H. Lichter-Marck	9/6/2018	PRJNA673739 SAMN16622088
Perityle intricata (Brandegee) Shinners	CAS 519263	USA: Nevada, NE Mercury, Nevada test site	CAS	J. Beatley	5/11/1965	PRJNA673739 SAMN16622089
Perityle intricata (Brandegee) Shinners	ILM 221	USA: California, San Bernardino co. Mohawk mtn.	UC	I.H. Lichter-Marck	9/2/2018	PRJNA673739 SAMN16622090
Perityle tenella (M.E. Jones) J.F. Macbr.	ILM 336	USA: Utah, Beaver Dam mtns	UC	I.H. Lichter-Marck	9/19/2018	PRJNA673739 SAMN16622091
Perityle specuicola S.L. Welsh & Neese	ILM 864	USA: Utah, Pipe canyon 20 miles north of Moab	UC	I.H. Lichter-Marck, S. Winitsky	8/30/2019	PRJNA673739 SAMN16622092
Perityle rupestris (A. Gray) Shinners var. *rupestris*	AZ 283476	United States, Texas, Jeff Davis, 5 miles north of Ft. Davis.	AZ	S. Sikes	9/3/65	PRJNA673739 SAMN16622093
Perityle rupestris (A. Gray) Shinners var.	UC 1440573	USA: Texas, Brewster co. Chaney Ranch	UC	A.M. Powell	7/14/64	PRJNA673739 SAMN16622094

Appendix I Continued

Taxon	Accession or collection #	Location	Herbarium	Collector(s)	Collection date	GenBank SRA #
albiflora A.M. Powell						
Perityle rupestris (A. Gray) Shinners var. *rupestris*	ILM 815	USA: Texas, Davis co. Davis mtns.	UC	I.H. Lichter-Marck	9/29/2019	PRJNA673739 SAMN16622095
Perityle rupestris (A. Gray) Shinners var. *albiflora* A.M. Powell	ILM 437	USA: Texas, Chisos mtns	UC	I.H. Lichter-Marck	10/4/2018	PRJNA673739 SAMN16622096
Perityle cinerea (A. Gray) A.M. Powell	UC 1391483	USA: Texas, Upton co. 10 mi S. of Rankin	UC	D.S. Correll, M.C. Johnston	6/14/1961	PRJNA673739 SAMN16622097
Perityle cinerea (A. Gray) A.M. Powell	Powell1310	USA: Texas, Pecos, 7-Mile Mesa, caprocks at southeast end, all exposures; near Fort Stockton.	SRSC	A.M. Powell	9/15/64	PRJNA673739 SAMN16622098
Perityle cernua (Greene) Shinners	Lundell 2402	USA: Dona Ana co. Mouth of Long Canyon	Lundell	R.M. Spellenberg, T.K. Todsen	9/27/1970	PRJNA673739 SAMN16622099
Perityle huecoensis A.M. Powell	UC 1609992	Mexico: Chihuahua, Mcpio. Juarez, Sierra Juarez on the west side of Cd. Juarez.	UC	R.M. Spellenberg, L. Brouillet, D. Kearns	5/29/1993	PRJNA673739 SAMN16622100
Perityle fosteri A. Powell	UTH 6528	USA: Texas, Apache mtns., Panther cyn.	UTH	J.F. Weedin	7/4/1978	PRJNA673739 SAMN16622101
Perityle carmenensis A.M. Powell	UTH 59919	Mexico: Coahuila, Sierra del Carmen	UTH	R. Spellenberg	8/7/1989	PRJNA673739 SAMN16622102
Perityle carmenensis A.M. Powell	Spellenberg 9960	Mexico, Coahuila, Extremo NE, Sierra el Carmen ca. 20 air miles S of U.S. border, ca 1 km N of Campo Dos in N-S running Cañón el Moreno (=Cn. Dos; Cn. Corte Madera)	SRSC	R. W. Spellenberg	7/7/89	PRJNA673739 SAMN16622103
Perityle vitreomontana Warnock	CAS 884918	USA: Texas, Webster co. Glass mtns, east of Alpine	CAS	A.M. Powell	6/20/1978	PRJNA673739 SAMN16622104
Perityle vitreomontana Warnock	Powell4956	USA: Texas, Brewster, Glass Mountains, Gilliland Canyon, upper slopes and bluffs, NE exposures.	SRSC	A.M. Powell	10/6/84	PRJNA673739 SAMN16622105
Perityle lindheimeri (A. Gray) Shinners	UC 1440574	USA: Val Verde co., Carruther's creek, 8 miles south of Loma Alta	UC	A.M. Powell, S. Sikes	6/19/1965	PRJNA673739 SAMN16622106
Perityle castillonii I.M. Johnst.	Lundell 59901	Mexico: Coahuila, Canon de Indio Felipe	Lundell	Robert M. Stewart	6/14/1941	PRJNA673739 SAMN16622107
Perityle dissecta (Torr.) A. Gray	CAS 1073859	USA: Texas, Presidio co., Chinati mtns.	CAS	E.J. Scott, S.P. Rankin, M.L. Butterwick, P.R. Manning	6/17/2004	PRJNA673739 SAMN16622108
Perityle dissecta (Torr.) A. Gray	SRSC	USA: Texas, Presidio co., Chinati mtns.	SRSC	A. Black, M. Eason S.N.	8/11/2019	PRJNA673739 SAMN16622109
Perityle bisetosa (Torr. ex. A. Gray) Shinners	UC 1412751	USA: Texas, Brewster co., Black Gap Wildlie refuge	UC	D.S. Correll, H. Correll	11/9/1967	PRJNA673739 SAMN16622110

Appendix I Continued

Taxon	Accession or collection #	Location	Herbarium	Collector(s)	Collection date	GenBank SRA #
var. *scalaris*						
Perityle bisetosa (Torr. ex. A. Gray) Shinners var. *bisetosa*	ILM 840	USA: Texas, Terell co. Sanderson	UC	I.H. Lichter-Marck	9/25/2019	PRJNA673739 SAMN16622111
Perityle parryi A. Gray	UC 1729590	USA: Texas, Presidio, Big Bend Ranch State Natural Area	UC	G. Webster	10/11/1997	PRJNA673739 SAMN16622112
Perityle parryi A. Gray	ILM 433a	USA: Texas, Brewster co. Lajitas	UC	I.H. Lichter-Marck	10/5/2018	PRJNA673739 SAMN16622113
Perityle vaseyi J.M. Coult.	AZ 416297	USA: Texas, Brewster, Plateau south of Cigar Mountain, along Hwy 170, 0.8 km west of Terlingua Creek crossing at Study Butte	AZ	M. Fishbein, A. Rein, L. Worcester	8/14/13	PRJNA673739 SAMN16622114
Perityle aglossa A. Gray	UC 1326735	USA: Texas, Brewster co., Santa Elena cyn.	UC	D.S. Correll, H.B. Correll	11/11/1967	PRJNA673739 SAMN16622115
Perityle aglossa A. Gray	ILM 451	USA: Texas, Brewster co., Boquillas cyn.	UC	I.H. Lichter-Marck	10/7/2018	PRJNA673739 SAMN16622116
Perityle angustifolia (A. Gray) Shinners	UC 1391720	USA: Texas, Val Verde co. Eagle nest canyon	UC	D.S. Correll	5/9/1967	PRJNA673739 SAMN16622117
Perityle angustifolia (A. Gray) Shinners	ILM 453	USA: Texas, Val Verde co., Eagle nest bridge.	UC	I.H. Lichter-Marck	10-7-2018	PRJNA673739 SAMN16622118
Perityle jaliscana A. Gray	CAS 420809	Mexico: Jalisco, Mpio. Zapopan, Sierra San Esteban	CAS	A. Garcia-Guerrero, M. Dolores	2/8/1994	PRJNA673739 SAMN16622119
Perityle incompta Brandegee	UC1787460	Mexico: Baja California Sur, Agua Verde.	UC	Jon. P. Rebman, J. Emming, M. White	10/9/2003	PRJNA673739 SAMN16622120
Conoclinium coelestinum (L.) DC		USA: Falls Church, VA	UC	Funk V.A.	2001-09-11	PRJNA540287 SAMN11585391
Eutrochium fistulosum (Barratt) E.E. Lamont		USA: Virginia, Fairfax Co., cultivated	US	Funk V.A.	2015-09-25	PRJNA540287 SAMN11585392
Chromolaena corymbosa (Aubl.) R.M. King and H. Rob		British Virgin Islands: Tortolla	US	Funk V.A.	1994-02-03	PRJNA540287 SAMN11585390
Stevia sp.		Argentina: La Rioja Provice	US	Funk V.A. & Bonifacino J.M.	2016-03-07	PRJNA540287 SAMN11585393
Helianthus annuus L.		Greenhouse grown seed, USDA, PI 603989	NA	Unknown	2014	PRJNA540287 SAMN11585423